# Probing anomalous $tbW$ couplings in single-top production using top polarization at the Large Hadron Collider

**Saurabh D. Rindani and Pankaj Sharma**

*Theoretical Physics Division, Physical Research Laboratory,*
*Navrangpura, Ahmedabad 380 009, India*

*E-mail:* saurabh@prl.res.in, pankajs@prl.res.in

Abstract: We study the sensitivity of the Large Hadron Collider (LHC) to anomalous $tbW$ couplings in single-top production in association with a $W^-$ boson followed by semileptonic decay of the top. We calculate top polarization and the effects of these anomalous couplings to it at two centre-of-mass (cm) energies of $7\,\mathrm{TeV}$ and $14\,\mathrm{TeV}$. As a measure of top polarization, we look at various laboratory frame distributions of its decay products, viz., lepton angular and energy distributions and $b$-quark angular distributions, without requiring reconstruction of the rest frame of the top, and study the effect of anomalous couplings on these distributions. We construct certain asymmetries to study the sensitivity of these distributions to anomalous $tbW$ couplings. The $Wt$ single-top production mode helps to isolate the anomalous $tbW$ couplings in contrast to top-pair production and other single-top production modes, where other new-physics effects can also contribute. We find separate limits on real and imaginary parts of the dominant anomalous coupling $f_{2R}$ which may be obtained by utilizing these asymmetries at the LHC.

Keywords: Beyond Standard Model, Heavy Quark Physics

# Contents

## 1 Introduction

Since the discovery of the top quark at Tevatron [1], its properties have been studied extensively, in particular its mass [2]. With a mass $m_t = 172.6 \pm 1.4\,\mathrm{GeV}$ close to the electroweak (EW) scale, the top quark is widely considered to be a key to the understanding of the mechanism of electroweak symmetry breaking. Owing to its large mass, its decay width $\Gamma_t = 1.3\,\mathrm{GeV}$ is large, leading to an extremely short life time, $\tau_t = 1/\Gamma_t \simeq 5 \times 10^{-25}$ s. This is an order of magnitude smaller than the hadronization time scale $\tau_{had} \simeq 1/\Lambda_{QCD} \sim 3 \times 10^{-24}$ s, and hence it decays before any non-perturbative effects can spoil its spin information. As a consequence, its polarization can be determined through the angular and/or energy distributions of its decay products [3]. The degree of polarization of the top quark may be a probe of any new physics responsible for its production. Top-quark polarization has been suggested for the study of new physics models in top-pair as well as single-top production at hadron colliders [4–8].

At the Large Hadron Collider (LHC), top quarks will be produced mainly in pairs dominantly through gluon fusion whose contribution to the cross section is 90%, while quark-antiquark annihilation contributes 10%. Both these production mechanisms proceed mainly through QCD interactions. Since gluon couplings are chirality-conserving, the

polarization of top quarks can arise only through the $Z$-exchange contribution to $q\bar{q}$ annihilation channel, and is expected to be very small. However, single-top production can also occur [9–16, 19, 22–25], and has already been seen [26]. Since it proceeds via weak interactions, top quarks will have large polarization [15, 16]. At LHC energies, single-top quark events in the SM are expected to be produced via a) the $t$-channel ($bq \to tq'$) process, b) the $s$-channel process ($q\bar{q}' \to t\bar{b}$) and c) the $tW$ associated production process ($bg \to tW^-$) [13]. In all these processes, there is at least one chiral vertex which gives rise to large top polarization. The three processes are completely different kinematically and can be separated from each other. In this work, we study in detail the effect of anomalous $tbW$ vertex on top polarization in associated production of the top quark with a $W$ boson.

Among all top couplings to gauge and Higgs bosons, the $tbW$ vertex deserves special attention since the top quark is expected to decay almost completely via this interaction. However, in several extensions of SM, as for example supersymmetry and models of dynamical symmetry breaking, sizable deviations are possible from the SM predictions and also new decays of top quarks are possible. These deviations of the $tbW$ vertex may be observed in top decays. Single-top production is another source to study deviation in the $tbW$ vertex. For on-shell top, bottom and $W$, the most general effective vertices for the $tbW$ interaction up to dimension five can be written as [27]

$$V_{t \to bW^+} = \frac{-g}{\sqrt{2}} V_{tb} \left[ \gamma^\mu (\mathrm{f}_{1L} P_L + \mathrm{f}_{1R} P_R) - \frac{i\sigma^{\mu\nu}}{m_W} (p_t - p_b)_\nu (\mathrm{f}_{2L} P_L + \mathrm{f}_{2R} P_R) \right] \tag{1.1}$$

for the decay $t \to bW^+$, and

$$V_{b \to tW^-} = \frac{-g}{\sqrt{2}} V_{tb}^* \left[ \gamma^\mu (\mathrm{f}_{1L}^* P_L + \mathrm{f}_{1R}^* P_R) - \frac{i\sigma^{\mu\nu}}{m_W} (p_t - p_b)_\nu (\mathrm{f}_{2R}^* P_L + \mathrm{f}_{2L}^* P_R) \right] \tag{1.2}$$

for $tW^-$ production from a virtual $b$, where $V_{tb}$ is the Cabibbo-Kobayashi-Maskawa matrix element, and $\mathrm{f}_{1L}$, $\mathrm{f}_{2L}$, $\mathrm{f}_{1R}$, $\mathrm{f}_{2R}$ are couplings. In the SM, $\mathrm{f}_{1L} = 1$ and $\mathrm{f}_{1R} = \mathrm{f}_{2L} = \mathrm{f}_{2R} = 0$. We have assumed all the anomalous couplings to be complex and treat real and imaginary parts of these couplings as independent parameters. We assume CP to be conserved in this analysis. Various extensions of the SM would have specific predictions for these anomalous couplings. For example, the contributions to these form factors in two Higgs doublet model (2HDM), minimal supersymmetric standard model (MSSM) and top-color assisted Technicolor model (TC2) have been evaluated in ref. [28].

Tevatron provides the only existing direct limits on anomalous $tbW$ couplings through $W$ polarization measurements. Recently, CDF II with $2.7\,\mathrm{fb}^{-1}$ of collected data reported results for the longitudinal and right-handed helicity fractions of the $W$ boson in semileptonic top-decays [17]. D0 also reported results on $W$ helicity fractions using a combination of semileptonic and dilepton decay channels [18]. These results on $W$ polarization measurements led to a limit of $[-0.3,\ 0.3]$ on $\mathrm{f}_{2R}$ at the 95% confidence level (CL) [19] in single-top production. The CMS and ATLAS collaborations have also reported the $W$ helicity fractions with early LHC data [20, 21]. In ref. [22], the authors have used the recent top quark decay asymmetries from ATLAS and the $t$-channel single-top cross section from CMS to put the limits on $tbW$ couplings. They find that despite the small statistics available, the early LHC limits of $[-0.6,\ 0.3]$ on $\mathrm{f}_{2R}$ are not too far from the Tevatron limits.

Apart from direct measurements at the LHC and Tevatron, there are stringent indirect constraints coming from low-energy measurements of anomalous $tbW$ couplings. The measured rate of $b \to s\gamma$ puts stringent constraints on the couplings $f_{1R}$ and $f_{2L}$ of about $4 \times 10^{-3}$, since their contributions to $B$-meson decay get an enhancement factor of $m_t/m_b$ [29–32]. The bound on the anomalous coupling $f_{2R}$ is very weak, $[-0.15, 0.57]$ at 95 % CL [32]. In ref. [33], a slightly more stringent bound has been found on $f_{2R}$ utilizing $B_{d,s} - \bar{B}_{d,s}$ mixing. These bounds are obtained by taking one coupling to be non-zero at a time. However if one allows all couplings to be non-zero simultaneously, there is a possibility of cancellations among contributions of different couplings and the limits on these couplings could be very different.

Single-top production in association with a $W^-$ boson can be used to probe the size and nature of the $tbW$ couplings. Apart from the cross section, the angular distribution of the top, and even the polarization of the top would give additional information enabling the determination of the $tbW$ coupling. Here we focus on the polarization of the top produced in the $tW$ associated production process. The most direct way to determine top polarization is by measuring the angular distribution of its decay products in its rest frame. However, at the LHC reconstructing the top rest frame is difficult and will result in large systematic uncertainties. In this paper, we show how the decay lepton angular distributions in the laboratory (lab) frame can be a useful probe of top polarization and hence of anomalous $tbW^-$ couplings.

In this context it is interesting to recall that the angular distribution of the charged lepton is independent of anomalous $tbW$ couplings in the decay of the top quark, to linear order in the anomalous couplings (the "decoupling theorem") [34–41]. Hence, the lepton angular distribution may be considered to be a pure and robust probe of any new physics involved in the production of the top quark. In this analysis, we study the angular distribution of the charged lepton without making the approximation that anomalous couplings are small and include higher-order terms in anomalous couplings. We also study the distributions to linear order in the anomalous couplings in the region of validity of the decoupling theorem. In this way, we investigate the range of anomalous couplings for which the decoupling theorem is valid. We find that the azimuthal distribution of the lepton is sensitive to top polarization and can be used to probe the form factor $f_{2R}$. The use of laboratory-frame charged-lepton azimuthal distribution for the measurement of top polarization in $t\bar{t}$ production at the LHC in a certain class of $Z'$ models was demonstrated in [6].

While charged-lepton angular distributions, at least for small values of anomalous couplings, would be a direct measure of top polarization, and hence would probe anomalous $tbW$ couplings in $tW^-$ production, other kinematic distributions could also be used to study anomalous $tbW$ couplings. Thus, the charged-lepton energy distribution and the decay-$b$ angular distribution, which do not obey the decoupling theorem, would depend on top polarization as well as anomalous couplings in top decay. Thus they would get contributions from $tbW$ couplings in production as well as in decay. We have thus also studied the charged-lepton energy distribution and the $b$-quark angular distribution as probes of anomalous $tbW$ couplings. In all cases, we obtain analytical expressions for the parton-level distributions at leading order in the couplings.
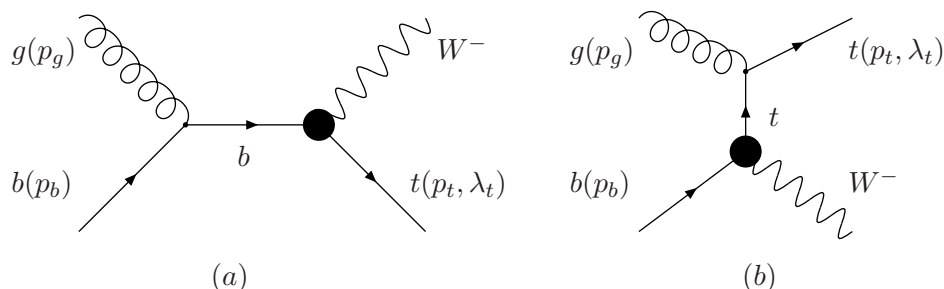
**Figure 1**. Feynman diagrams contributing to associated $tW^-$ production at the LHC.

The effects of top polarization in $tW$ and $tH^-$ production have been studied previously in [4, 42]. Ref. [42] included the effects of one-loop EW SUSY corrections. It did not however include top decay. Top polarization in different modes of single-top production has also been studied in [14, 15], where spin-sensitive variables were used to analyze effective left- and right-handed couplings of the top coming from physics beyond the SM.

The rest of the paper is organized as follows. In the next section we discuss the cross section for single-top production in association with a $W^-$, the corresponding top angular distribution, as well as top polarization in the process, obtaining analytical expressions and evaluating them numerically. In section 3, we obtain expressions for charged-lepton angular and energy distributions, and in section 4 we obtain the $b$-quark angular distribution. In case of each distribution, we evaluate an asymmetry as a variable sensitive to $tbW$ anomalous couplings. Section 5 contains an analysis of the sensitivities of the various asymmetries to the anomalous couplings. In section 6 we discuss briefly the backgrounds and non-leading corrections to our signal process, and conclude in section 7. The appendix contains certain lengthy mathematical expressions.

## 2    Single-top production in association with a $W$ boson

As stated earlier, single-top production at hadron colliders occurs through three different modes. All these three modes are distinct in terms of initial and final states and are in principle separately measurable. The $tW^-$ mode of single-top production is distinct from other two modes in the sense that it is affected by the new physics only in the $tbW$ vertex while, in other modes, there may be exotic scalars or gauge bosons which can give additional contributions to the process. The $tW^-$ mode of single-top production has been studied in detail in refs. [13, 23, 24]. At the parton level, the $tW^-$ production proceeds through a gluon and a bottom quark each coming from a proton and gets contribution from two diagrams. Feynman diagrams for the process $g(p_g)b(p_b) \rightarrow t(p_t, \lambda_t)W^-$ are shown in figure 1, where $\lambda_t = \pm 1$ represent the top helicity and the blobs denote effective $tbW$ vertices, including anomalous couplings, in the production process. These couplings are also involved in the decay of the top as shown in figure 2.
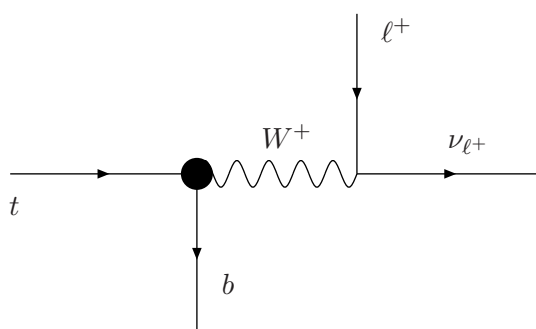
**Figure 2**. Anomalous $tbW$ couplings in top decay.

We obtain analytical expressions for the spin density matrix for $tW$ production including anomalous couplings. Use was made of the analytic manipulation program FORM [43]. We find that at linear order, only the real part of the coupling $f_{2R}$ gives significant contribution to the production density matrix, whereas contributions from all other couplings are proportional to the mass of $b$ quark (which we neglect consistently) and hence vanish in the limit of zero bottom mass. To second order in anomalous couplings, other anomalous couplings do contribute, but we focus only on $f_{2R}$, since its contribution, arising at linear order, is dominant. Expressions for the spin density matrix elements $\rho(\pm, \pm)$ and $\rho(\pm, \mp)$ for $tW$ production, where $\pm$ are the signs of the top-quark helicity, are given in the appendix.

## 2.1 Production cross section

After convoluting the density matrix given in the appendix with parton distribution functions and integrating it over the phase space, the diagonal elements of this integrated density matrix, which we denote by $\sigma(+, +)$ and $\sigma(-, -)$, are respectively the cross sections for the production of positive and negative helicity tops and $\sigma_{\text{tot}} = \sigma(+, +) + \sigma(-, -)$ is the total cross section.

For numerical calculations, we use the leading-order parton distribution function (PDF) sets of CTEQ6L [44] with a factorization scale of $m_t = 172.6\,\text{GeV}$. We also evaluate the strong coupling at the same scale, $\alpha_s(m_t) = 0.1085$. We make use of the following values of other parameters: $M_W = 80.403\,\text{GeV}$, the electromagnetic coupling $\alpha_{em}(m_Z) = 1/128$ and $\sin^2 \theta_W = 0.23$. We set $f_{1L} = 1$ and $V_{tb} = 1$ in our calculations. We take only one coupling to be non-zero at a time in the analysis, except in section 5.

In figure 3, we show the cross section as a function of various anomalous $tbW$ couplings for two different values of centre-of-mass (cm) energies of $7\,\text{TeV}$ and $14\,\text{TeV}$ for which the LHC is planned to operate. We show contributions of anomalous couplings to the cross section at linear order as well as without the approximation. From figure 3, one can infer that the cross section is very sensitive to negative values of $\text{Re}f_{2R}$. The linear approximation is seen to be good for values of anomalous coupling ranging from $-0.05$ to $0.05$.

Since the cross section may receive large radiative corrections at the LHC, we focus on using observables like asymmetries which are ratios of some partial cross sections, and which are expected to be insensitive to such corrections.
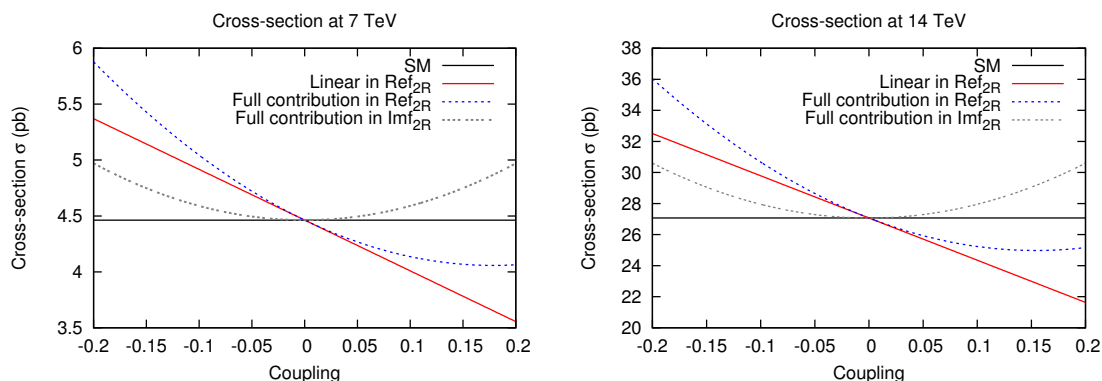
**Figure 3**. The cross section for $tW^-$ production at the LHC for two different cm energies, 7 TeV (left) and 14 TeV (right), as a function of anomalous $tbW$ couplings.
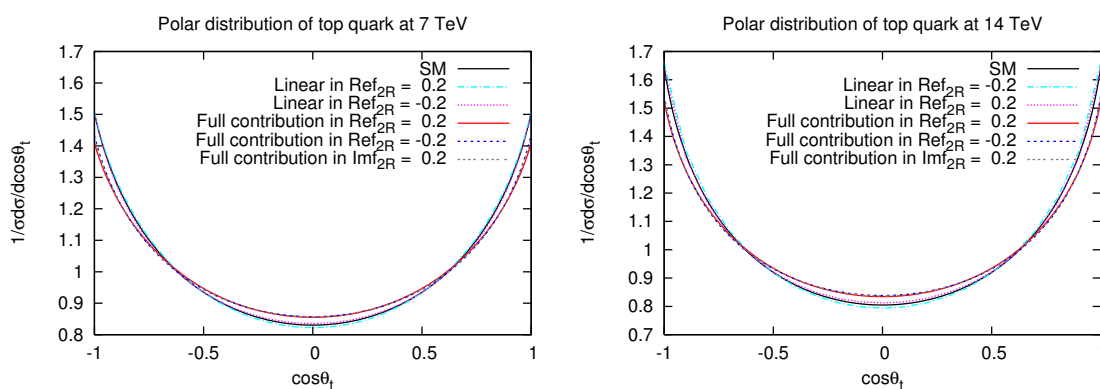


**Figure 4**. The top-polar angular distributions for $tW^-$ production at the LHC for two different cm energies, 7 TeV (left) and 14 TeV (right), for different anomalous $tbW$ couplings.

## 2.2 Top-angular distribution

The angular distribution of the top quark would be modified by anomalous couplings. Since the top quark is produced in a $2 \to 2$ process, its azimuthal distribution is flat. We can study its polar distribution with the polar angle defined with respect to either of the beam directions as the $z$ axis. We find that the polar distribution is sensitive to anomalous $tbW$ couplings. The normalized polar distribution is plotted in figure 4 for cm energies 7 TeV and 14 TeV.

As can be seen from figure 4, the curves for the polar distributions for the SM and for the anomalous couplings of magnitude 0.2 are separated from each other. The top distribution has no forward-backward asymmetry, the colliding beams being identical. However, we can define an asymmetry utilizing the polar distributions of the top quark as

$$\mathcal{A}_\theta^t = \frac{\sigma(|z| > 0.5) - \sigma(|z| < 0.5)}{\sigma(|z| > 0.5) + \sigma(|z| < 0.5)} \tag{2.1}$$

where $z$ is $\cos\theta_t$. We plot this asymmetry as a function of anomalous $tbW$ couplings for two cm of energies $\sqrt{s} = 7$ TeV and 14 TeV in figure 5. $A_\theta^t$ deviates more than $1\sigma$ from its
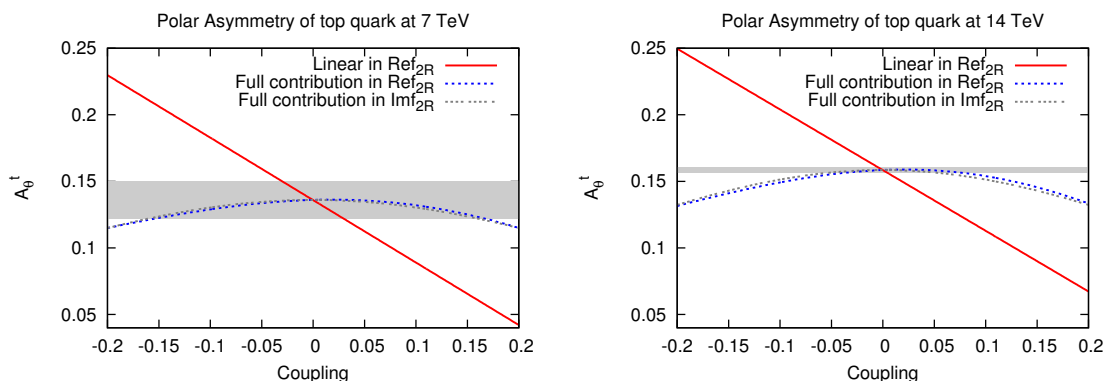
**Figure 5**. The top polar asymmetries for $tW^-$ production at the LHC for two different cm energies, 7 TeV (left) and 14 TeV (right), as a function of anomalous $tbW$ couplings. The grey band corresponds to the top-polar asymmetry predicted in the SM with a $1\,\sigma$ error interval.

SM value for $\mathrm{Ref}_{2R}$ and $\mathrm{Imf}_{2R}$ close to $\pm 0.2$ for $\sqrt{s} = 7\,\mathrm{TeV}$, but is much more sensitive for $\sqrt{s} = 14\,\mathrm{TeV}$.

The asymmetry $\mathcal{A}_\theta^t$ requires accurate determination of the top direction in the lab frame and a quantitative estimate of its sensitivity to anomalous couplings needs details of the efficiency of reconstruction of the direction. We do not study this asymmetry any further, but proceed to a discussion of top polarization.

### 2.3 Top polarization

The degree of longitudinal polarization $P_t$ of the top quark is given by

$$P_t = \frac{\sigma(+,+) - \sigma(-,-)}{\sigma(+,+) + \sigma(-,-)}. \tag{2.2}$$

This polarization asymmetry is shown in figure 6 as a function of anomalous couplings in the linear approximation, as well as without approximation, for $\sqrt{s} = 7\,\mathrm{TeV}$ and $14\,\mathrm{TeV}$. As compared to the SM value of $-0.256$ for $\sqrt{s} = 14\,\mathrm{TeV}$, the degree of longitudinal top polarization varies from $-0.07$ to $-0.281$ for $\mathrm{Ref}_{2R}$ varied over the range $-0.2$ to $+0.2$, while it varies from $-0.139$ to $-0.256$ for the same range of $\mathrm{Imf}_{2R}$, and is symmetric about $\mathrm{Imf}_{2R} = 0$.

We notice that just as for the total cross section, $P_t$ is more sensitive to negative values of $\mathrm{Ref}_{2R}$. Also, $P_t$ is equally sensitive to negative and positive values of $\mathrm{Imf}_{2R}$. Thus $P_t$ can be a very good probe of $\mathrm{Ref}_{2R}$ and $\mathrm{Imf}_{2R}$ if it can be measured at the LHC. However, the standard measurement of $P_t$ requires reconstruction of the top rest frame which is a difficult task, and would entail reduction in efficiency. We will therefore investigate lab frame decay distributions for the measurement of anomalous couplings.

All the quantities considered so far, viz., the total cross section, the top polar distribution and the top polarization, can only be measured using information from the decay of the top. Both the polar distribution and the top polarization would play a role in determining the distributions of the decay products. Our main aim is to devise observables which can be measured in the lab frame and give a good estimate of top polarization and
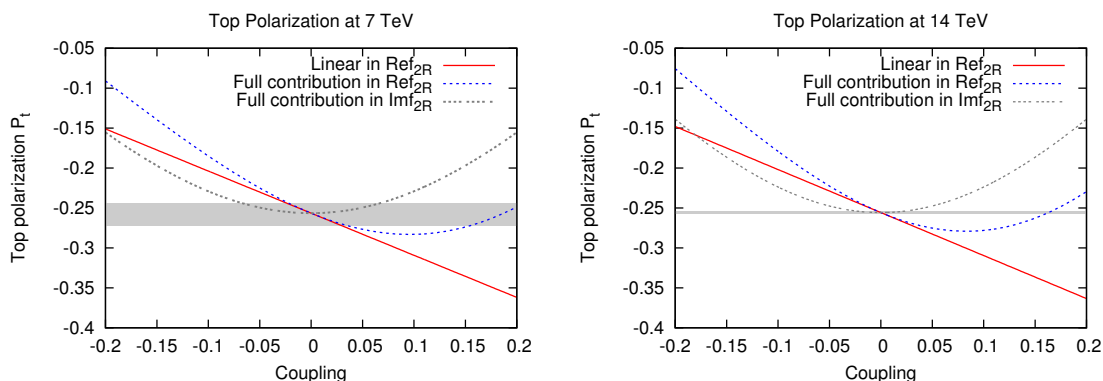
**Figure 6**. The top polarization asymmetry for $tW^-$ production at the LHC for two different cm energies, $7\,\text{TeV}$ (left) and $14\,\text{TeV}$ (right), as a function of anomalous $tbW$ couplings. The grey band corresponds to the top-polarization asymmetry predicted in the SM with a $1\,\sigma$ error interval.

thence probe anomalous $tbW$ couplings in single-top production. We proceed to construct such observables from kinematic variables of the charged lepton and $b$ quark produced in the decay of the top.

## 3 Charged-lepton distributions

Top polarization can be determined by the angular distribution of its decay products. In the SM, the dominant decay mode is $t \to bW^+$, with a branching ratio (BR) of 0.998, with the $W^+$ subsequently decaying to $\ell^+\nu_\ell$ (semileptonic decay, BR 1/9 for each lepton) or $u\bar{d}$, $c\bar{s}$ (hadronic decay, BR 2/3). The angular distribution of a decay product $f$ for a top-quark ensemble has the form

$$\frac{1}{\Gamma_f}\frac{\mathrm{d}\Gamma_f}{\mathrm{d}\cos\theta_f} = \frac{1}{2}(1 + \kappa_f P_t \cos\theta_f). \tag{3.1}$$

Here $\theta_f$ is the angle between fermion $f$ and the top spin vector in the top rest frame and $P_t$ (defined in eq. (2.2)) is the degree of polarization of the top-quark ensemble. $\Gamma_f$ is the partial decay width and $\kappa_f$ is the spin analyzing power of $f$. Obviously, a larger $\kappa_f$ makes $f$ a more sensitive probe of the top spin. The charged lepton and the $d$ quark are the best spin analyzers with $\kappa_{\ell^+} = \kappa_{\bar{d}} = 1$, while $\kappa_{\nu_\ell} = \kappa_u = -0.30$ and $\kappa_b = -\kappa_{W^+} = -0.39$, all $\kappa$ values being at tree level [45]. Thus the $\ell^+$ or $d$ have the largest probability of being emitted in the direction of the top spin and the least probability in the direction opposite to the spin. Since at the LHC, lepton energy and momentum can be measured with high precision, we focus on leptonic decays of the top.

To preserve spin coherence while combining top production with decay, we make use of the spin density matrix formalism. Since $\Gamma_t/m_t \sim 0.008$, we can use the narrow width approximation (NWA) to write the cross section in terms of the product of the $2 \to 2$ production density matrix $\rho$ and the decay density matrix $\Gamma$ of the top as

$$\overline{|\mathcal{M}|^2} = \frac{\pi\delta(p_t^2 - m_t^2)}{\Gamma_t m_t}\sum_{\lambda,\lambda'}\rho(\lambda, \lambda')\Gamma(\lambda, \lambda'). \tag{3.2}$$

where and $\lambda, \lambda' = \pm 1$ denote (the sign of) the top helicity.

The top production spin density matrix $\rho(\lambda, \lambda')$ for process $gb \to tW^-$ is given in appendix. We obtain the top decay density matrix $\Gamma(\lambda, \lambda')$ for the process $t \to bW^+ \to b\ell^+\nu_\ell$ including anomalous $tbW$ couplings and write it in a Lorentz invariant form. We find

$$
\begin{aligned}
\Gamma(\pm, \pm) = g^4 \; |\Delta(p_W^2)|^2 [m_t^2 - 2(p_t \cdot p_\ell)] \Big[ |f_{1L}|^2 \Big\{ (p_t \cdot p_\ell) \mp m_t(p_\ell \cdot n_3) \Big\} \\
+ \mathrm{Re} f_{1L} f_{2R}^* \Big\{ m_t m_W \mp \frac{m_t^2 + m_W^2}{m_W}(p_\ell \cdot n_3) \mp \frac{2}{m_W}(p_b \cdot n_3)(p_t \cdot p_\ell) \Big\} \\
+ \frac{|f_{2R}|^2}{2} \Big\{ m_W^2 + \frac{m_t^2 - 2 p_t \cdot p_\ell}{2} \mp 2 \left[(p_\ell \cdot n_3) + (p_b \cdot n_3)\right] \Big\} \Big],
\end{aligned} \tag{3.3}
$$

for the diagonal elements and

$$
\begin{aligned}
\Gamma(\mp, \pm) = g^4 \; |\Delta(p_W^2)|^2 [m_t^2 - 2(p_t \cdot p_\ell)] \Big[ |f_{1L}|^2 \left\{ -m_t[p_\ell \cdot (n_1 \mp i n_2)] \right\} \\
- \mathrm{Re} f_{1L} f_{2R}^* \Big\{ \frac{m_t^2 + m_W^2}{m_W}[p_\ell \cdot (n_1 \mp i n_2)] - \frac{2}{m_W}[p_b \cdot (n_1 \mp i n_2)](p_t \cdot p_\ell) \Big\} \\
- |f_{2R}|^2 \Big\{ [(p_\ell + p_b) \cdot (n_1 \mp i n_2)] \Big\} \Big],
\end{aligned} \tag{3.4}
$$

for the off-diagonal ones. Here $\Delta(p_W^2)$ is the $W$ boson propagator, for which we will use the narrow-width approximations for our numerical calculations, and $n_i^\mu$'s $(i = 1, 2, 3)$ are spin four-vectors for the top with four-momentum $p_t$, corresponding to rest-frame spin quantization axes $x$, $y$ and $z$ respectively, with the properties $n_i \cdot n_j = -\delta_{ij}$ and $n_i \cdot p_t = 0$. In the top rest frame they take the standard form $n_i^0 = 0$, $n_i^k = \delta_i^k$.

The full details of the factorization of the differential cross section for top production followed by its decay in a generic production process into production and decay parts is given in ref. [41]. Here we use the same formalism for single-top production and its decay and write the partial cross section in the parton cm frame as

$$
d\sigma = \frac{1}{32(2\pi)^4 \Gamma_t m_t} \int \left[ \sum_{\lambda, \lambda'} \frac{d\sigma(\lambda, \lambda')}{d\cos\theta_t} \left( \frac{\langle \Gamma(\lambda, \lambda') \rangle}{p_t \cdot p_\ell} \right) \right] d\cos\theta_t \; d\cos\theta_\ell \; d\phi_\ell \; E_\ell dE_\ell \; dp_W^2, \tag{3.5}
$$

where the $b$-quark energy integral is replaced by an integral over the invariant mass $p_W^2$ of the $W$ boson, its polar-angle integral is carried out using the Dirac delta function of eq. (3.2), and the average over its azimuthal angle is denoted by the angular brackets. $d\sigma(\lambda, \lambda')/d\cos\theta_t$ is proportional to $\rho(\lambda, \lambda')$, with the normalization chosen so that $d\sigma(\lambda, \lambda)/d\cos\theta_t$ is the differential cross section for the $2 \to 2$ process of $tW^-$ production with helicity index $\lambda$ of the top.

## 3.1 Angular distributions of charged leptons

We evaluate top decay in the rest frame of the top quark with the $z$ axis as the spin quantization axis, which would also be the direction of the boost required to go to the parton cm frame. In the rest frame of the top quark, the diagonal and off-diagonal elements of decay density matrix, after averaging over the azimuthal angle of $b$ quark w.r.t. the plane

of top and lepton momenta, are given by

$$\langle\Gamma(\pm,\pm)\rangle = g^4 m_t E_\ell^0 |\Delta_W(p_W^2)|^2 (m_t^2 - 2p_t\cdot p_\ell)\Bigg[\left\{|f_{1L}|^2 + \mathrm{Re}f_{1L}f_{2R}^*\frac{m_t\,m_W}{p_t\cdot p_\ell}\right\}(1\pm\cos\theta_\ell^0)$$

$$-|f_{2R}|^2\left(1-\frac{m_t^2+m_W^2}{2p_t\cdot p_\ell}\right)(1\mp\cos\theta_\ell^0)\pm|f_{2R}|^2\frac{m_W^2 m_t^2}{2(p_t\cdot p_\ell)^2}\cos\theta_\ell^0\Bigg], \tag{3.6}$$

$$\langle\Gamma(\pm,\mp)\rangle = g^4 m_t E_\ell^0 |\Delta_W(p_W^2)|^2 (m_t^2 - 2p_t\cdot p_\ell)\sin\theta_\ell^0 e^{\pm i\phi_\ell^0}\Bigg[|f_{1L}|^2 + \mathrm{Re}f_{1L}f_{2R}^*\frac{m_t\,m_W}{p_t\cdot p_\ell}$$

$$+|f_{2R}|^2\left\{1-\frac{m_t^2+m_W^2}{2p_t\cdot p_\ell}+\frac{m_W^2 m_t^2}{2(p_t\cdot p_\ell)^2}\right\}\Bigg], \tag{3.7}$$

where averaging over the azimuthal angle of the $b$ quark w.r.t. the plane of top and lepton momenta, denoted by angular brackets, is most conveniently carried out in a coordinate system defined with the $z$ axis along the lepton momentum direction.

In the limit of small anomalous coupling $f_{2R}$, we see from eqs. (3.6) and (3.7) that if we drop quadratic terms in $f_{2R}$, $\langle\Gamma(\lambda,\lambda')\rangle$ factorizes into a pure angular part $\mathcal{A}(\lambda,\lambda')$, which depends on helicities, and a lepton-energy dependent part which does not depend on the helicities, where

$$\mathcal{A}(\pm,\pm) = (1\pm\cos\theta_\ell^0), \qquad \mathcal{A}(\pm,\mp) = \sin\theta_\ell^0 e^{\pm i\phi_\ell^0}. \tag{3.8}$$

The factorization of $\langle\Gamma(\lambda,\lambda')\rangle$ into $\mathcal{A}(\lambda,\lambda')$ and a helicity-independent part in the rest frame of the top quark implies that since the corrections from anomalous couplings reside in the helicity-independent part, they are identical to those of the total width appearing in the denominator of the angular distribution, and cancel. This leads to the result of [34–41] that the energy averaged lepton angular distributions are insensitive to the new physics in top-quark decay in any top production process.

We study the angular distribution of the charged lepton in the lab frame both in the linear approximation of the anomalous couplings as well as with full contributions of the anomalous couplings without approximation.

We first obtain the angular distribution of the charged lepton in the parton cm frame, by integrating over the lepton energy, with limits given by $m_W^2 < 2(p_t\cdot p_\ell) < m_t^2$. This integral can be done analytically, giving the following expression for the differential cross section in the parton cm frame:

$$\frac{d\sigma}{d\cos\theta_t\,d\cos\theta_\ell\,d\phi_\ell} = \frac{1}{32\,\Gamma_t m_t}\,\frac{1}{(2\pi)^4}\int\left[\sum_{\lambda,\lambda'}\frac{d\sigma(\lambda,\lambda')}{d\cos\theta_t}g^4\mathcal{A}'(\lambda,\lambda')\right]|\Delta(p_W^2)|^2 dp_W^2, \tag{3.9}$$

where

$$\mathcal{A}'(\pm,\pm) = \frac{m_t^6}{24(1-\beta_t\cos\theta_{t\ell})^3 E_t^2}\Big[(1-r^2)^2\big\{(1\pm\cos\theta_{t\ell})(1\mp\beta_t)\left[|f_{1L}|^2(1+2r^2)+6r\mathrm{Re}f_{1L}f_{2R}^*\right]$$

$$+|f_{2R}|^2(2+r^2)(1\mp\cos\theta_{t\ell})(1\pm\beta_t)\big\}$$

$$\mp 12r^2|f_{2R}|^2\left(1-r^2+2\log r\right)(\cos\theta_{t\ell}-\beta_t)\Big], \tag{3.10}$$
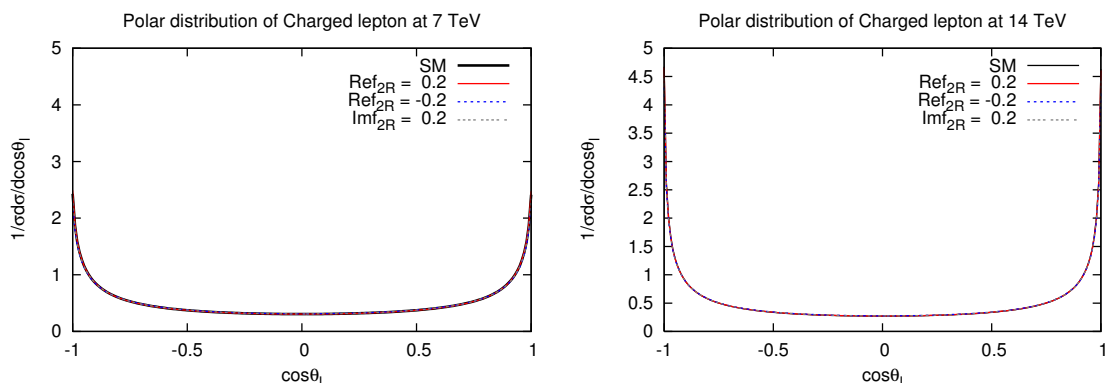
**Figure 7**. The normalized polar distribution of the charged lepton in $tW^-$ production at the LHC for two different cm energies, 7 TeV (left) and 14 TeV (right), for different anomalous $tbW$ couplings.

$$\mathcal{A}'(\pm, \mp) = \frac{m_t^7}{24(1 - \beta_t \cos\theta_{t\ell})^3 E_t^3} \sin\theta_{t\ell} e^{\pm i\phi_\ell} \Big[ (1 - r^2)^2 \{ |\mathrm{f}_{1L}|^2 (1 + 2r^2) + 6r \ \mathrm{Re}\mathrm{f}_{1L}\mathrm{f}_{2R}^*$$
$$- |\mathrm{f}_{2R}|^2 (2 + r^2) \} - 12r^2 \ |\mathrm{f}_{2R}|^2 \left( 1 - r^2 + 2\log r \right) \Big]. \tag{3.11}$$

Here $r = m_W/m_t$ and $\cos\theta_{t\ell}$ is the angle between the top quark and the charged lepton from the top decay in the parton cm frame, given by

$$\cos\theta_{t\ell} = \cos\theta_t \cos\theta_\ell + \sin\theta_t \sin\theta_\ell \cos\phi_\ell, \tag{3.12}$$

where $\theta_\ell$ and $\phi_\ell$ are the lepton polar and azimuthal angles.

In the lab frame, the lepton polar angle is defined w.r.t. either of the beam direction and the azimuthal angle is defined with respect to the top-production plane chosen as the $x$-$z$ plane, with beam direction as the $z$ axis and the convention that the $x$ component of the top momentum is positive. At the LHC, which is a symmetric collider, it is not possible to define a positive direction of the $z$ axis. Hence lepton angular distribution is symmetric under interchange of $\theta_\ell$ and $\pi - \theta_\ell$ as well as of $\phi_\ell$ and $2\pi - \phi_\ell$. The lab frame expression for the differential cross section is obtained from eq. (3.9) by an appropriate Lorentz transformation and integration over the parton densities.

We first look at the polar distribution of the charged lepton and the effect on it of anomalous $tbW$ couplings. As can be seen from figure 7, where we plot the polar distribution for two cm of the LHC energies $\sqrt{s} = 7$ TeV and 14 TeV, the normalized distributions are insensitive to anomalous $tbW$ couplings.

We next look at the contributions of anomalous couplings to the azimuthal distribution of the charged lepton. In figure 8, we show the normalized azimuthal distribution of the charged lepton in a linear approximation of the couplings for $\sqrt{s} = 7$ TeV and 14 TeV for different values of $\mathrm{Re}\mathrm{f}_{2R}$. At linear order, contributions of all other couplings vanish in the limit of vanishing bottom mass. In figure 9, we show the normalized azimuthal distribution of the charged lepton including higher-order terms in the couplings for $\sqrt{s} = 7$ TeV and 14 TeV for different values of $\mathrm{Re}\mathrm{f}_{2R}$ and $\mathrm{Im}\mathrm{f}_{2R}$. We see that the curves for real and imaginary parts of the anomalous coupling $\mathrm{f}_{2R}$ peak near $\phi_\ell = 0$ and $\phi_\ell = 2\pi$. The

**Figure 8**. The normalized azimuthal distribution of the charged lepton in $tW^-$ production at the LHC for two different cm energies, 7 TeV (left) and 14 TeV (right), for different anomalous $tbW$ couplings in the linear approximation. $\mathrm{Im}f_{2R}$ does not contribute in the linear order.
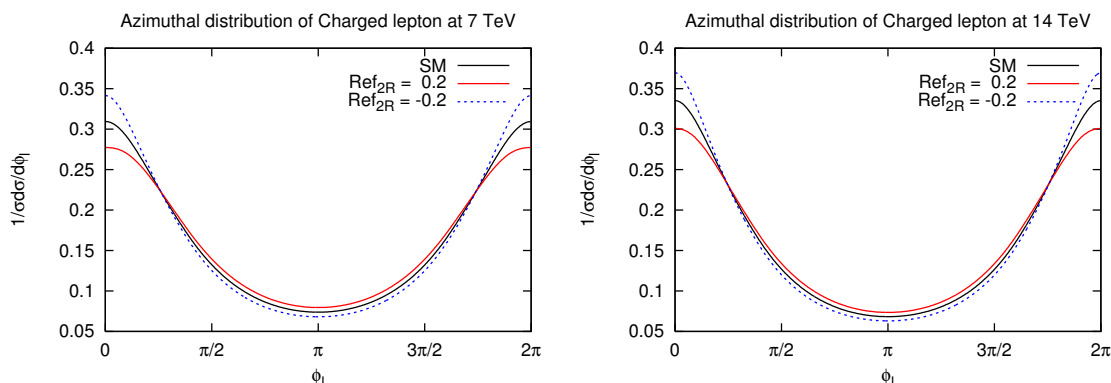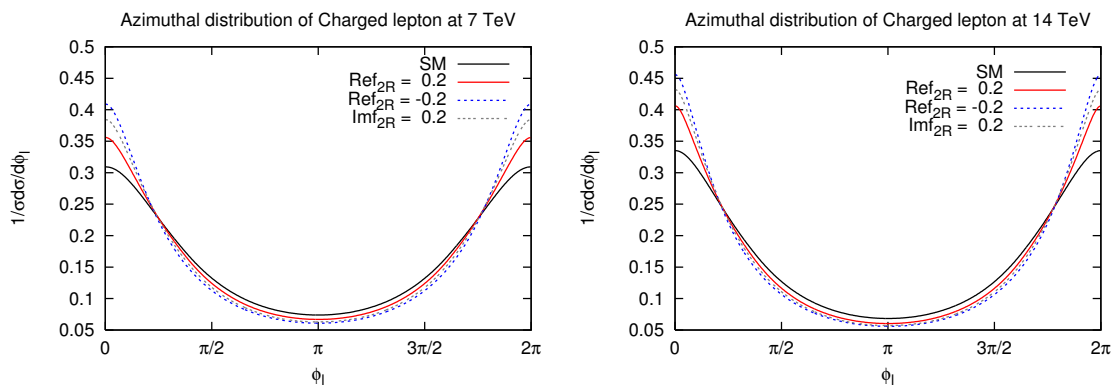


**Figure 9**. The normalized azimuthal distribution of the charged lepton in $tW^-$ production at the LHC for two different cm energies, 7 TeV (left) and 14 TeV (right), for different anomalous $tbW$ couplings without the linear approximation.

curves are well separated at the peaks for the chosen values of the anomalous $tbW$ couplings and are also well separated from the curve for the SM. We define an azimuthal asymmetry for the lepton to quantify these differences in the distributions by

$$A_\phi = \frac{\sigma(\cos\phi_\ell > 0) - \sigma(\cos\phi_\ell < 0)}{\sigma(\cos\phi_\ell > 0) + \sigma(\cos\phi_\ell < 0)}, \tag{3.13}$$

where the denominator is the total cross section. Plots of $A_\phi$ as a function of the couplings with and without cuts on the lepton momenta are shown in figure 10 for a cm energy of 7 TeV. In the former case, the rapidity and transverse momentum acceptance cuts on the decay lepton that we have used are $|\eta| < 2.5$, $p_T^\ell > 20\,\mathrm{GeV}$. The corresponding plots at $\sqrt{s} = 14\,\mathrm{TeV}$ with and without lepton cuts are shown in the figure 11. The lepton cuts increase the value of $A_\phi$ for the SM from 0.35 to around 0.45, and also increase $A_\phi$ substantially with anomalous couplings included. However, the cuts result in the reduction of signal events and from the figures 10 and 11, we see that these cuts actually decrease the sensitivity to anomalous couplings.
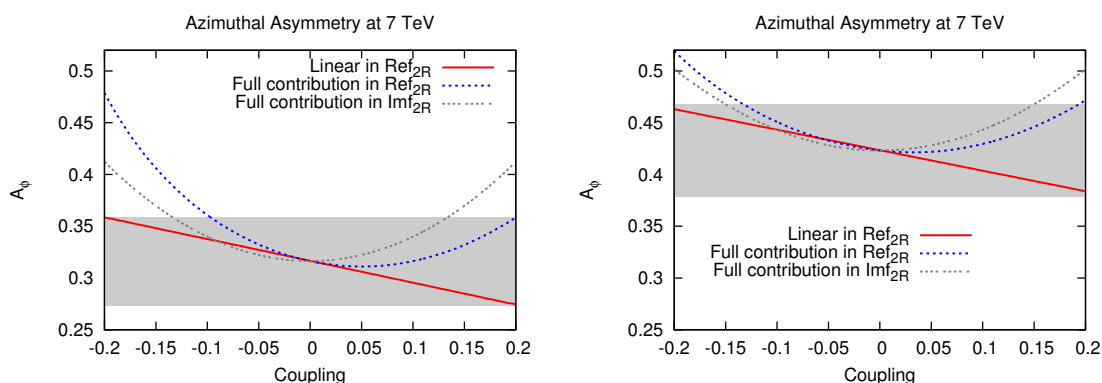
**Figure 10**. The azimuthal asymmetries of the charged lepton in $tW^-$ production at the LHC for cm energy 7 TeV without lepton cuts (left) and with cuts (right), as a function of anomalous $tbW$ couplings. The grey band corresponds to the azimuthal asymmetry predicted in the SM with 1 $\sigma$ error interval.
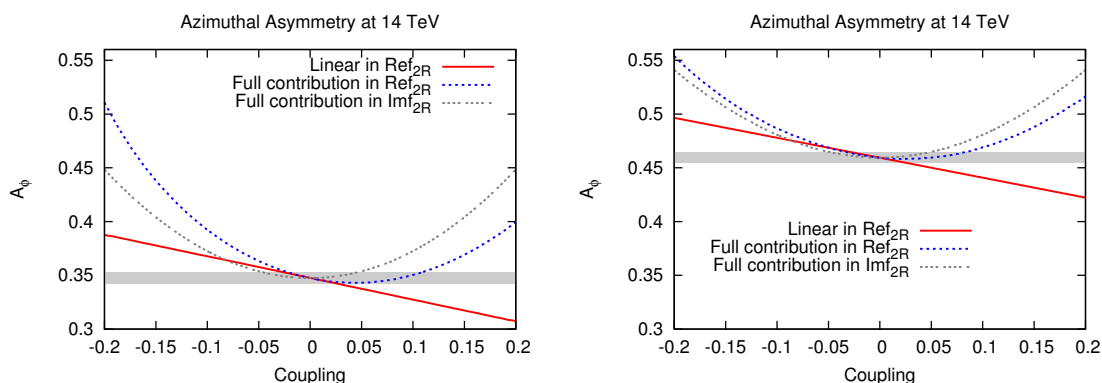


**Figure 11**. The azimuthal asymmetries of the charged lepton in $tW^-$ production at the LHC for cm energy 14 TeV without lepton cuts (left) and with cuts (right), as a function of anomalous $tbW$ couplings. The grey band corresponds to the azimuthal asymmetry predicted in the SM with a $1\sigma$ error interval.

The azimuthal distribution depends both on top polarization and on a kinematic effect. According to eq. (3.1), the decay lepton is emitted preferentially along the top spin direction in the top rest frame, with $\kappa_f = 1$. The corresponding distributions in the parton cm frame are given by eq. (3.9) with the angular parts described by eqs. (3.10) and (3.11). The rest-frame forward (backward) peak corresponds to a peak for $\cos\theta_{t\ell} = \pm 1$, as seen from the factor $(1 \pm \cos\theta_{t\ell})$ in the numerator of eq. (3.10). This is the effect of polarization. The kinematic effect is seen in the factor $(1 - \beta_t \cos\theta_{t\ell})^3$ in the denominator of eqs. (3.10) and (3.11), which again gives rise to peaking for large $\cos\theta_{t\ell}$. Eq. (3.12) therefore implies peaking for small $\phi_\ell$. This is borne out by the numerical results.

## 3.2 Energy distribution of charged leptons

We now study the energy distribution $d\sigma/dE_\ell$ of charged leptons to probe anomalous $tbW$ couplings in single-top production and decay. In the rest frame of the top quark, the
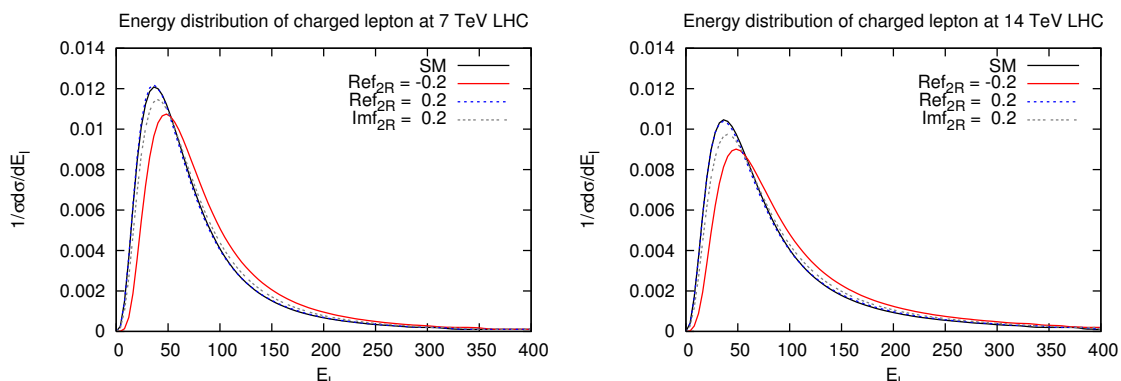
**Figure 12**. The energy distribution of the charged lepton in $tW^-$ production at the LHC for cm energies 7 TeV (left) TeV and 14 TeV (right) for different anomalous $tbW$ couplings.

$E_\ell$ distribution of the decay density matrix $\Gamma(\lambda, \lambda')$ depends only on the combination of helicities, $(\lambda, \lambda')$. To linear order in the couplings, only the angular part of $\Gamma(\lambda, \lambda')$ depends on the helicities, and the energy dependence is the same for all helicity combinations, and is determined by the effective couplings occurring in decay. However, there is a weak dependence on the production differential cross section introduced because the boost to the parton cm frame is determined by $\theta_{t\ell}$. Thus, the $E_\ell$ distribution arises mainly from the decay process, and depends only weakly on the polarization.

We plot in figure 12 the $E_\ell$ distribution for $\sqrt{s} = 7$ and 14 TeV. We see that the distribution is peaked at low values of $E_\ell$ around 40-45 GeV, and all curves intersect at a particular value of $E_\ell \approx 62$ GeV. We also observe that the $E_\ell$ distribution is mainly sensitive to Ref$_{2R}$.

As seen from figure 12, the $E_\ell$ distribution is very sensitive to negative values of Ref$_{2R}$ and shows little sensitivity for positive values. The $E_\ell$ distribution at 7 TeV is peaked slightly more as compared to that for 14 TeV LHC, though the position of the peak for both is about the same.

The curves for the $E_\ell$ distribution for anomalous $tbW$ couplings of $\pm 0.2$ and the SM are well separated from each other and intersect at $E_\ell^C = 62$ GeV. To quantify this difference and to make better use of statistics, we construct an asymmetry around the intersection point of the curves, defined by

$$A_{E_\ell} = \frac{\sigma(E_\ell < E_\ell^C) - \sigma(E_\ell > E_\ell^C)}{\sigma(E_\ell < E_\ell^C) + \sigma(E_\ell > E_\ell^C)}, \tag{3.14}$$

where the denominator is the total cross section. Plots for $A_{E_\ell}$ as a function the coupling are shown in figure 13 for two cm energies of 7 TeV and 14 TeV. We can see from the figure that $A_{E_\ell}$ is very sensitive to Ref$_{2R}$ and hence can be a sensitive probe of this coupling. It is also seen from the figure that the $A_{E_\ell}$ for the SM is positive for $\sqrt{s} = 7$ TeV, but negative for $\sqrt{s} = 14$ TeV. This is in accordance with a sharper peaking of the energy distribution in the former case. Another difference between the asymmetries for the two cm energies is that $A_{E_\ell}$ changes sign with the sign for some value of Ref$_{2R}$ in case of $\sqrt{s} = 7$ TeV, but remains negative in case of $\sqrt{s} = 14$ TeV.
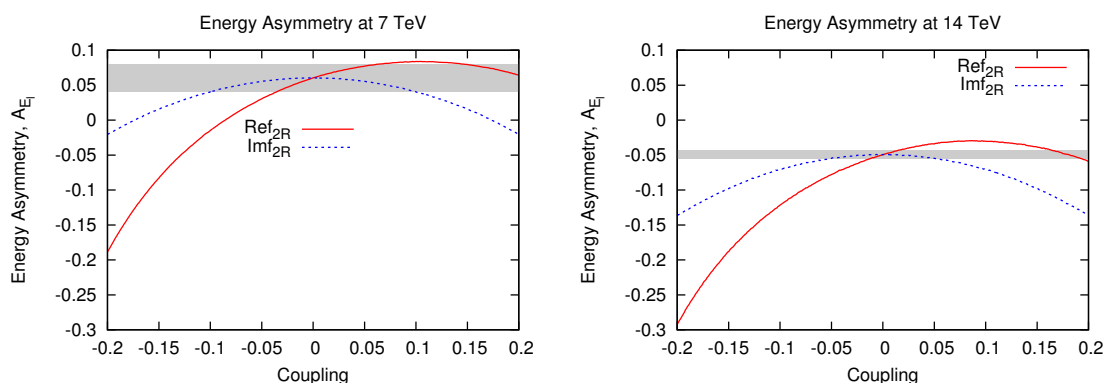
**Figure 13**. The energy asymmetry of the charged lepton in $tW^-$ production at the LHC for cm energy 14 TeV without lepton cuts (left) and with cuts (right), as a function of anomalous $tbW$ couplings. The grey band corresponds to the energy asymmetry predicted in the SM with a $1\sigma$ error interval.

## 4 Angular distribution of $b$ quarks

Although the charged-lepton azimuthal distribution provides a neat way to probe top polarization independent of new physics in the top-decay vertex, it suffers from low branching ratio of $W$ and hence low number of events for the analysis. This situation can be improved upon by using $b$-quark angular distributions, without restricting only to the leptonic decays of the $W$ coming from top decay, and thus utilizing all the single-top events. We thus assume, for purposes of this section, that the top quark can be identified in hadronic and semi-leptonic decays with sufficiently good efficiency to enable measurement of $b$-quark distribution in all of them.

As described earlier, we use NWA to factorize the full process into single-top production and top decay. Similar to eq. (3.5), we can write the full differential cross section for the process $g(p_g)b(p_b) \to t(p_t, \lambda_t)W^-$ followed by $t(p_t, \lambda_t) \to b(p'_b)W^+$ as

$$\frac{d\sigma}{d\cos_{\theta_t} d\Omega_b} = \frac{1}{128(2\pi)^3 \hat{s}^{3/2}} \frac{|\overrightarrow{p_t}|}{\Gamma_t m_t} \frac{(m_t^2 - m_W^2)}{E_t^2(1 - \beta_t \cos \theta_{bt})^2} \sum_{\lambda_t, \lambda'_t} \left[ \rho(\lambda_t, \lambda'_t) \Gamma(\lambda_t, \lambda'_t) \right], \quad (4.1)$$

where the polar angle $\theta_t$ of the top quark, and the polar and azimuthal angles $\theta_b$ and $\phi_b$ of the $b$ quark produced in top decay, are measured with respect to the parton direction as the $z$ axis, and with the $xz$ plane defined as the plane containing the top momentum. $\theta_{bt}$ is the angle between the top momentum and the momentum of the decay $b$ quark.

The density matrix for single-top production $\rho(\lambda_t, \lambda'_t)$ appearing in eq. (4.1) is given in the appendix. The decay density matrix for $t \to bW$ in the top-quark rest frame is given by[1]

$$\Gamma(\pm, \pm) = \frac{g^2 m_t^2}{2} \left[ \mathcal{C}_1 \pm \mathcal{C}_2 \cos \theta_b^0 \right], \quad (4.2)$$

$$\Gamma(\pm, \mp) = \frac{g^2 m_t^2}{2} \left[ \mathcal{C}_2 \sin \theta_b^0 e^{\pm \phi_b^0} \right], \quad (4.3)$$

---

[1]The expressions for charged-lepton and $b$-quark angular distributions agree with those given in ref. [49].
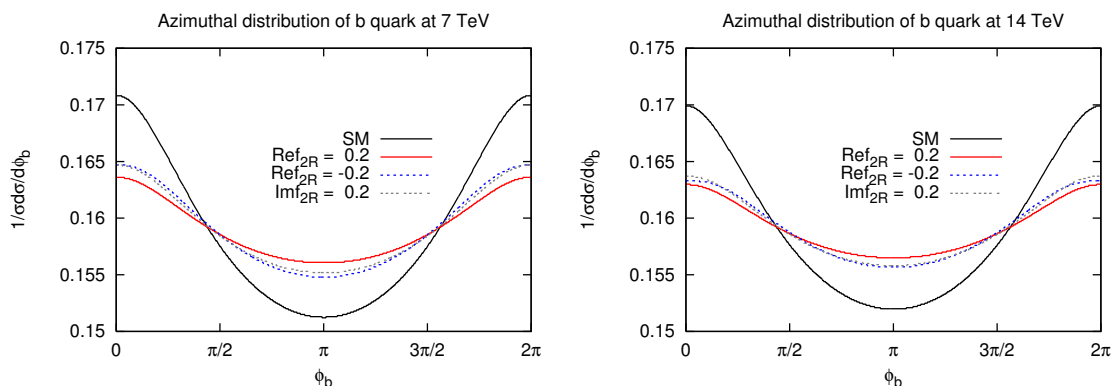
**Figure 14**. The azimuthal distribution of the $b$ quark in $tW^-$ production at the LHC for cm energies 7 TeV and 14 TeV for different anomalous $tbW$ couplings.

where

$$\mathcal{C}_1 = \frac{1}{2r^2}(1 - r^2)\left[|f_{1L}|^2(2r^2 + 1) + \mathrm{Re}f_{1L}f_{2R}^* \, 6r + |f_{2R}|^2(2 + r^2)\right], \tag{4.4}$$

$$\mathcal{C}_2 = \frac{1}{2r^2}(1 - r^2)\left[|f_{1L}|^2(2r^2 - 1) + \mathrm{Re}f_{1L}f_{2R}^* \, 2r + |f_{2R}|^2(2 - r^2)\right]. \tag{4.5}$$

The rest frame polar and azimuthal angles of the $b$, respectively $\theta_b^0$ and $\phi_b^0$, may be expressed in terms of the parton cm frame angles in a straightforward way.

Plots for the azimuthal distribution of the $b$ quark for different values of anomalous couplings $\mathrm{Re}f_{2R}$ and $\mathrm{Im}f_{2R}$ are shown in figure 14. The curves for values $\pm 0.2$ of these couplings are well separated from each other and from the SM curve. In the azimuthal distribution of the $b$ quark, we get dependence on anomalous couplings both from production as well as decay. We find that the contributions from production and from decay come with opposite signs, partially cancelling each other.

To study the sensitivity and make the best use of azimuthal $b$-quark distribution, we construct an asymmetry $A_b$:

$$A_b = \frac{\sigma(\cos\phi_b > 0) - \sigma(\cos\phi_b < 0)}{\sigma(\cos\phi_b > 0) + \sigma(\cos\phi_b < 0)}. \tag{4.6}$$

The asymmetry $A_b$ is plotted in figure 15 as a function of anomalous couplings for the cm energies $\sqrt{s} = 7$ TeV and 14 TeV. From the figure it is clear that $A_b$ shows less sensitivity to couplings $\mathrm{Re}f_{2R}$ and $\mathrm{Im}f_{2R}$ as compared to other asymmetries. As stated earlier, this is due to the fact that the contributions of anomalous couplings to the asymmetry from the production and the decay are of opposite in sign and hence tend to cancel each other.

## 5 Sensitivity analysis for anomalous *tbW* couplings

We now study the sensitivities of the observables discussed in the previous sections to the anomalous $tbW$ couplings at the LHC running at two cm of energies viz., 7 TeV and 14 TeV, with integrated luminosities 1 fb$^{-1}$ and 10 fb$^{-1}$, respectively. To obtain the $1\sigma$ limit on the anomalous $tbW$ couplings from a measurement of an observable, we find those values
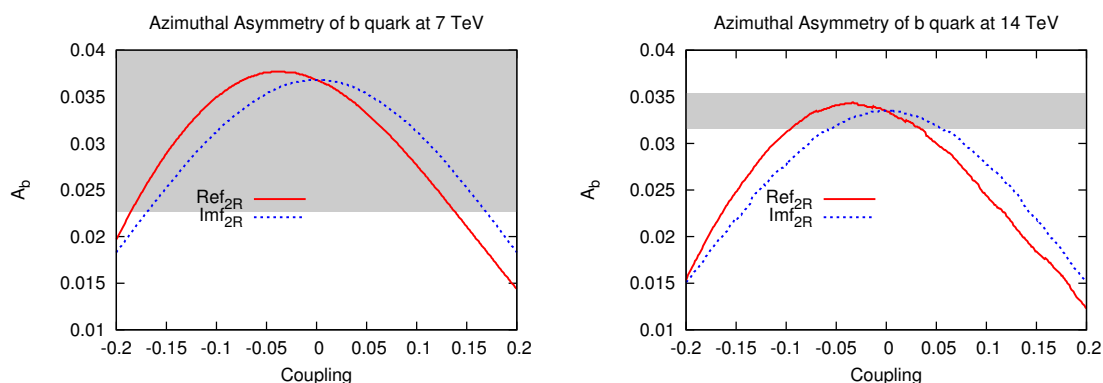
**Figure 15**. The azimuthal asymmetry of the $b$ quark in $tW^-$ production at the LHC for cm energies 7 TeV and 14 TeV as a function of anomalous $tbW$ couplings. The grey band corresponds to the asymmetry predicted in the SM with a $1\sigma$ error interval.

of the couplings for which observable deviates by $1\sigma$ from its SM value. The statistical uncertainty $\sigma_i$ in the measurement of any generic asymmetry $\mathcal{A}_i$ is given by

$$\sigma_i = \sqrt{\frac{1 - \left(\mathcal{A}_i^{SM}\right)^2}{\mathcal{N}}}, \qquad (5.1)$$

where $\mathcal{A}_i^{SM}$ is the asymmetry predicted in the SM and $\mathcal{N}$ is the total number of events predicted in the SM. We apply this to the various asymmetries we have discussed. In case of the top polarization asymmetry, the limits are obtained on the assumption that the polarization can be measured with 100% accuracy.

The $1\sigma$ limits on $Ref_{2R}$ and $Imf_{2R}$ are given in table 1 where we assume only one anomalous coupling to be non-zero at a time. We have also assumed measurements on a $tW^-$ final state. Including the $\bar{t}W^+$ final state will improve the limits by a factor of $\sqrt{2}$. In case of the lepton distributions, we take into account only one leptonic channel. Again, including other leptonic decays of the top would improve the limits further. The limits corresponding to a linear approximation in the couplings are denoted by the label "lin. approx.". Apart from the $1\sigma$ limits shown in table 1, which correspond to intervals which include zero value of the coupling, there are other disjoint intervals which could be ruled out if no deviation from the SM is observed for $P_t$ and $A_{E_\ell}$. This is apparent from figures 6 and 13. The additional allowed intervals for $Ref_{2R}$ from $P_t$ measurement are [0.158, 0.205] and [0.160, 0.167] for cm energies of 7 TeV and 14 TeV, respectively. The corresponding intervals for $A_{E_\ell}$ are [0.147, 0.285] and [0.175, 0.185].[2]

It is seen that the azimuthal asymmetry $A_\phi$ and the energy asymmetry $A_{E_\ell}$ of the charged lepton are more sensitive to negative values of the anomalous couplings $Ref_{2R}$. $A_{E_\ell}$ is the most sensitive of the asymmetries we consider. In fact, the sensitivity of $A_{E_\ell}$ to $Ref_{2R}$ and $Imf_{2R}$ is comparable to the sensitivity of top polarization to the same couplings, despite the fact that only one leptonic decay channel, with a branching fraction of about $1/9$, is considered for $A_{E_\ell}$. The additional contribution to $A_{E_\ell}$ of the $f_{2R}$ coupling through

---

[2][a, b] denotes the allowed values of the coupling $f$ at the $1\sigma$ level, satisfying $a < f < b$.

| | 7 TeV | | 14 TeV | |
|---|---|---|---|---|
| Observable | $\mathrm{Ref_{2R}}$ | $\mathrm{Imf_{2R}}$ | $\mathrm{Ref_{2R}}$ | $\mathrm{Imf_{2R}}$ |
| $P_t$ | $[-0.025, 0.032]$ | $[-0.072, 0.072]$ | $[-0.004, 0.004]$ | $[-0.034, 0.034]$ |
| $P_t$ (lin. approx.) | $[-0.027, 0.027]$ | $-$ | $[-0.004, 0.004]$ | $-$ |
| $A_\phi$ | $[-0.133, 0.194]$ | $[-0.150, 0.150]$ | $[-0.034, 0.086]$ | $[-0.050, 0.050]$ |
| $A_\phi$ (lin. approx.) | $[-0.204, 0.204]$ | $-$ | $[-0.030, 0.030]$ | $-$ |
| $A_b$ | $[-0.191, 0.147]$ | $[-0.177, 0.177]$ | $[-0.096, 0.035]$ | $[-0.059, 0.059]$ |
| $A_{E_\ell}$ | $[-0.044, 0.073]$ | $[-0.114, 0.114]$ | $[-0.006, 0.009]$ | $[-0.038, 0.038]$ |

**Table 1**. Individual limits on real and imaginary parts of anomalous coupling $f_{2R}$ which may be obtained by the measurement of the observables shown in the first column of the table at two cm of energies viz., 7 TeV and 14 TeV with integrated luminosities of 1 fb$^{-1}$ and 10 fb$^{-1}$ respectively. A dash "$-$" indicates that no limits are possible.

the top decay channel seems to compensate for the low branching fraction. $A_b$ is seen to have the lowest sensitivity, where there is partial cancellation of contributions to the asymmetry from production and from decay.

We also obtain simultaneous limits (taking both $\mathrm{Ref_{2R}}$ and $\mathrm{Imf_{2R}}$ non-zero simultaneously) on these anomalous couplings that may be obtained by combining the measurements of all observables. For this, we perform a $\chi^2$ analysis to fit all the observables to within $f\sigma$ of statistical errors in the measurement of the observable. We define the following $\chi^2$ function

$$\chi^2 = \sum_{i=1}^{n} \left( \frac{P_i - O_i}{\sigma_i} \right)^2, \tag{5.2}$$

where the sum runs over the $n$ observables measured and $f$ is the degree of the confidence interval. $P_i$'s are the values of the observables obtained by taking both anomalous couplings non-zero (and is a function of the couplings $\mathrm{Ref_{2R}}$ and $\mathrm{Imf_{2R}}$) and $O_i$'s are the values of the observables obtained in the SM. $\sigma_i$'s are the statistical fluctuations in the measurement of the observables, given in eq. (5.1).

In figure 16, we show the $1\sigma$, $2\sigma$ and $3\sigma$ regions in $\mathrm{Ref_{2R}}$-$\mathrm{Imf_{2R}}$ plane allowed by combined measurement of asymmetries $A_{E_\ell}$, $A_\phi$ and $A_b$ taken two at a time. For this, in the $\chi^2$ function of eq. (5.2), we have taken only two of the three observables at a time. From among the three combinations shown in figure 16, we find that the strongest simultaneous limits come from the combined measurement of $A_{E_\ell}$ and $A_\phi$, viz., [-0.01, 0.02] on $\mathrm{Ref_{2R}}$ and $[-0.05, 0.05]$ on $\mathrm{Imf_{2R}}$, at the $1\sigma$ level.

In figure 17, we show the $1\sigma$, $2\sigma$ and $3\sigma$ regions in $\mathrm{Ref_{2R}}$-$\mathrm{Imf_{2R}}$ plane allowed by combined measurement of all three asymmetries $A_{E_\ell}$, $A_\phi$ and $A_b$ simultaneously. We find that the combined measurement of all the observables provide the most stringent simultaneous limits on $\mathrm{Ref_{2R}}$ and $\mathrm{Imf_{2R}}$ of [-0.010, 0.015] and $[-0.04, 0.04]$ respectively at $1\sigma$. We find that the energy asymmetry $A_{E_\ell}$ plays a crucial role in determining the combined limits.

We now compare our results with those of other works on the determination of anomalous $tbW$ couplings at the LHC. Refs. [12, 14, 15, 22, 48–50], have studied single-top production at the LHC in the context of anomalous $tbW$ couplings. Boos et al. [12] find a
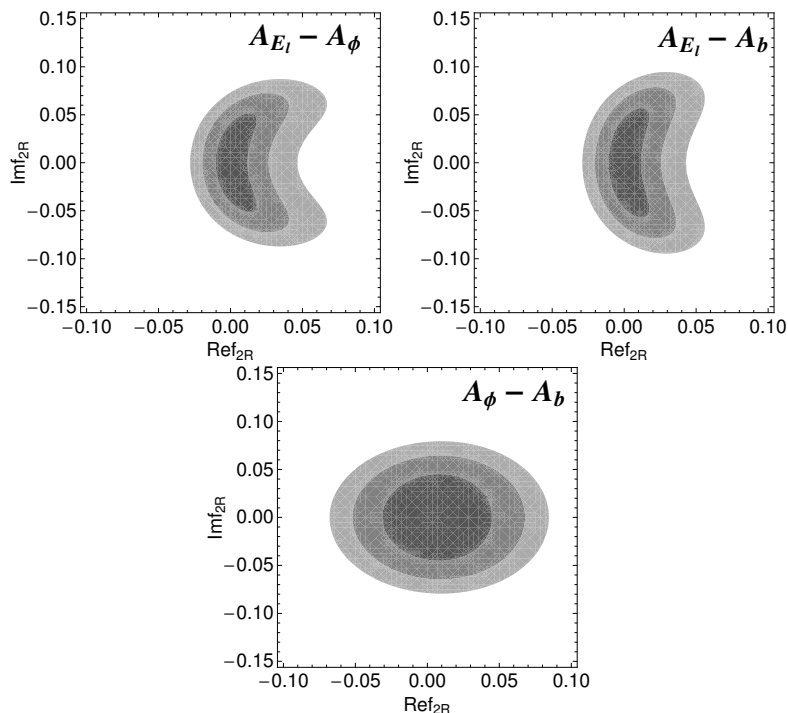
**Figure 16**. The $1\sigma$ (central region), $2\sigma$ (middle region) and $3\sigma$ (outer region) CL regions in the $Ref_{2R}$-$Imf_{2R}$ plane allowed by the combined measurement of two observables at a time. The left, centre and right plots correspond to measurements of the combinations $A_{E_\ell}$-$A_\phi$, $A_{E_\ell}$-$A_b$ and $A_\phi$-$A_b$ respectively. The $\chi^2$ values for $1\sigma$, $2\sigma$ and $3\sigma$ CL intervals are 2.30, 6.18 and 11.83 respectively for 2 parameters in the fit.
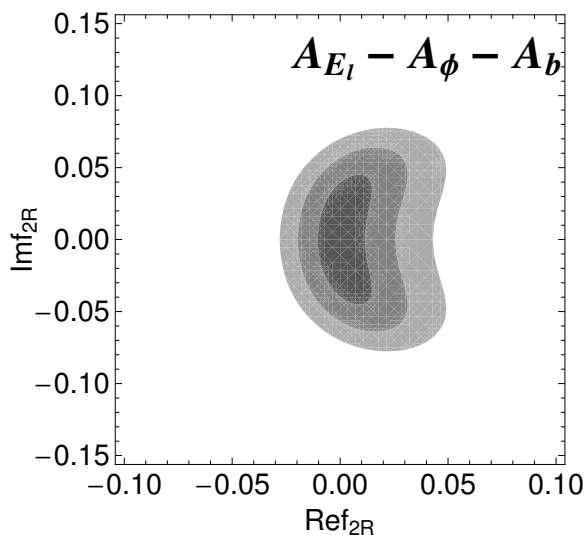


**Figure 17**. The $1\sigma$ (central region), $2\sigma$ (middle region) and $3\sigma$ (outer region) CL regions in the $Ref_{2R}$-$Imf_{2R}$ plane allowed by the combined measurement of all the observables simultaneously.

limit of $-0.12 < \text{f}_{2\text{R}} < 0.13$ at the LHC with $100\,\text{fb}^{-1}$ of luminosity. Refs. [14, 15] considered couplings $\text{f}_{1\text{L}}$ and $\text{f}_{1\text{R}}$ in their analysis and ignored $\text{f}_{2\text{R}}$ on which we focus. In ref. [48], the authors have studied all three single-top production channels to probe anomalous $tbW$ couplings and have utilized combinations of observables like cross sections, $W$ polarization helicity fractions in top decay, and other angular asymmetries. They predict a $1\sigma$ limit of $[-0.012, 0.024]$ on the coupling $\text{f}_{2\text{R}}$ with an integrated luminosity of $30\,\text{fb}^{-1}$. Ref. [49] determine expected $3\sigma$ limits on $\text{Ref}_{2\text{R}}$ to be $[-0.056, 0.056]$ and on $\text{Imf}_{2\text{R}}$ to be $[-0.115, 0.115]$, with $10\,\text{fb}^{-1}$ of integrated luminosity. Najafabadi [50] has studied the $tW$ channel for single-top production and determined the expected $1\sigma$ CL limits on anomalous coupling $\text{f}_{2\text{R}}$ to be in the range $[-0.026, 0.017]$ with $20\,\text{fb}^{-1}$ of integrated luminosity at $14\,\text{TeV}$ LHC using the single-top production cross section.

Refs. [27, 46, 47] have studied various observables in $t\bar{t}$ pair production at the LHC with semileptonic decays of the top. Ref. [27] predict $1\sigma$ limit on $\text{f}_{2\text{R}}$ of $[-0.019, 0.018]$ with $10\,\text{fb}^{-1}$ of integrated luminosity. Refs. [46, 47] study $W$ polarization in top decay in top-quark pair production at the LHC to constrain the anomalous $tbW$ couplings. They construct various asymmetries and helicity fractions to probe anomalous couplings in the decay of the top quark. Ref. [46] quotes a $2\sigma$ limit of $0.04$ on $\text{f}_{2\text{R}}$ with full detector-level simulations including systematic uncertainties and with different observables. Ref. [47] obtain a limit on $\text{f}_{2\text{R}}$ of $[-0.0260, 0.0312]$ with simulation of the ATLAS detector.

All these analyses except those of [27, 49] consider anomalous $tbW$ couplings to be real parameters. In our analysis, we consider all anomalous couplings to be complex and find that only the real part of the coupling $\text{f}_{2\text{R}}$ gives significant contribution to all observables at linear order in anomalous couplings. Without a linear approximation, other couplings also contributes at the quadratic level. However, we focus only on the $\text{f}_{2\text{R}}$ since its contribution is dominant, occurring as it does at linear order. With integrated luminosity $10\,\text{fb}^{-1}$ and cm energy $14\,\text{TeV}$, we find the most stringent limits possible on $\text{Ref}_{2\text{R}}$ to be $[-0.006, 0.009]$ and on $\text{Imf}_{2\text{R}}$ to be $\pm 3.8 \times 10^{-2}$, coming from the lepton energy asymmetry $A_{E_\ell}$, which are nominally an order of magnitude better than the Tevatron direct search limit and better than the limits obtained in refs. [12, 27, 46–49]. Our estimate $[-0.044, 0.073]$ for limits on $\text{Ref}_{2\text{R}}$ in the $\sqrt{s} = 7\,\text{TeV}$ run is comparable to the numbers obtained by the extrapolation of the result of [22] to an integrated luminosity of $1\,\text{fb}^{-1}$. It is of course true that including realistic detector efficiencies, especially for $b$ tagging, will worsen our limits somewhat. Moreover, additional kinematic cuts, needed for a separation of $Wt$ events from the background would also lead to a dilution of the limits. But, the crucial point in our analysis is that we are able to determine limits on real and imaginary parts of coupling $\text{f}_{2\text{R}}$ separately while others determine limits only on the magnitude of $\text{f}_{2\text{R}}$. Moreover, top-pair production could include effects of new particles in intermediate states, whereas our analysis isolates $tbW$ couplings, and is qualitatively different.

## 6 Backgrounds and next-to-leading-order corrections

It is worthwhile to examine the dominant backgrounds to our signal process $gb \to tW^-$. Background estimation and extraction of the signal for this process has been studied in

detail in refs. [13, 23, 51]. The main background for this signal would come from (a) processes which contain continuum of $W^+W^-b$ involving an off-shell top quark, (b) top-pair production where one of the $b$ quarks is missed as it lies outside the detector range, (c) processes containing $W^+W^-j$ where lighter-quark jet $j$ is misidentified as a $b$-quark jet (the probability being 1%). The contributions of the processes $W^+W^-b$ and $W^+W^-j$, which are of order $O(\alpha_s\alpha_W^2)$, are much smaller than the $tW^-$ signal, which is of order $O(\alpha_s\alpha_W)$. Tait [13] has considered both W's to decay leptonically and hence the final state consists of two hard charged leptons + one $b$ jet + missing $E_T$ (arising from two neutrinos). For such a signal, the process $ZZj$ would also act as background where one of the $Z$ decays into a pair of the charged leptons and the other $Z$ decays into neutrinos. In ref. [13], all the backgrounds are simulated at LO in the strong and weak couplings and standard acceptance cuts ($p_T > 15\,\mathrm{GeV}$ and $\eta < 2$) are applied on all final state particles. To suppress large $t\bar{t}$ background, it is required that there should not be more than one hard $b$ jet. After applying these cuts and with integrated luminosity less than 1 fb$^{-1}$ at 14 TeV LHC, the conclusion of the ref. [13] is that $5\sigma$ observation of single-top events in $tW^-$ channel is possible.

The authors of refs. [23, 51] consider the situation where the $W$ coming from the top quark decays leptonically and the other $W$ decays into two light-quark jets. Therefore the signal would consist of three jets, one of which is a hard $b$ jet, an isolated hard charged lepton and missing energy. The jet multiplicity requirement rejects a major part of the $t\bar{t}$ background. Also, the requirement of the two-jet invariant mass to be within the vicinity of the $W$ mass (70 GeV-90 GeV) eliminates all backgrounds which do not have another $W$, as for example $W$+jets, other single-top and QCD processes. In all these analyses, $b$-tagging efficiency is assumed to be 60%. After applying all the cuts, it has been shown that 10% sensitivity can be achieved with 1 fb$^{-1}$ by combining both electron and muon channels. Ref. [23] considers $Wt$ mode including NLO-QCD corrections and concludes that since the $Wt$ cross section is larger than the uncertainty in $t\bar{t}$ cross section, the $Wt$ channel is well-defined and is visible from backgrounds.

Turning to radiative corrections, NLO QCD corrections to the process $gb \to tW^-$ in the context of the 14 TeV LHC has been studied in detail in ref. [52]. These corrections are substantial, up to 70% of the LO cross section. They are shown to be dependent on the factorization scale and increase steadily with the increment in the scale. For factorization scale $\mu = \mu_0/2 = (m_t + m_W)/2$, the $K$ factor for the QCD correction is 1.4 while for $\mu = 2\mu_0 = 2(m_t + m_W)$, it is around 1.7. In our analysis, we have taken $\mu = m_t$, for which the $K$ factor is expected to be about 1.5.

The complete NLO EW corrections have been calculated in ref. [53] for $pp \to tW^- + X$ in the context of the LHC. The EW corrections are always positive and are maximum for $tW$ invariant mass closed to threshold value. With the increase in $tW$ invariant mass, these EW corrections decrease. So, the maximum EW correction is around 7% at threshold and it goes down to 3.5% for $tW$ invariant mass of 1200 GeV.

In our analysis, we have not included any $K$ factor. Including NLO factors in our analysis would not change the asymmetries much, but would increase the signal and hence, the sensitivity on anomalous couplings would be enhanced.

## 7 Summary and conclusions

We have investigated the sensitivity of the LHC to anomalous $tbW$ couplings in single-top production in association with a $W^-$ boson followed by semileptonic decay of the top. We derived analytical expressions for the spin density matrix of the top quark including contributions of both real and imaginary parts of the anomalous $tbW$ couplings. We find that in the limit of vanishing $b$ quark mass, only the real part of coupling $f_{2R}$ contributes to the spin density matrix at linear order. Because of the chiral structure of the anomalous $tbW$ couplings, the resulting top polarizations are vastly different from those expected in the SM. We find that substantial deviations, as much as 20-30%, in the degree of longitudinal top polarization from the SM value of $-0.256$ are possible even for anomalous couplings of magnitude 0.1. The degree of longitudinal top polarization varies from $-0.075$ to $-0.363$ for $\mathrm{Re}f_{2R}$ while for $\mathrm{Im}f_{2R}$ it is symmetric around the SM value and varies from $-0.139$ to $-0.256$ for the same range of $\mathrm{Im}f_{2R}$ as compared to the SM value of $-0.256$ for 14 TeV LHC.

Since top polarization can only be measured through the distributions of its decay products in top decay, we studied distributions of top decay products. We consider the top to decay semi-leptonically, since this channel is expected to have the best accuracy and spin analyzing power. However, decay distributions can get contributions from anomalous couplings responsible for top polarization as well as for top decay. We find that normalized charged-lepton azimuthal and energy distributions and $b$-quark azimuthal distributions are sensitive to anomalous couplings $\mathrm{Re}f_{2R}$ and $\mathrm{Im}f_{2R}$. In each case, we define an asymmetry, whose deviation from the SM value would be a measure of the anomalous couplings. We find that the azimuthal asymmetry $A_\phi$ and the energy asymmetry $A_{E_\ell}$ of the charged lepton are more sensitive to negative values of the anomalous couplings $\mathrm{Re}f_{2R}$. A limit of $[-0.034, 0.086]$ on $\mathrm{Re}f_{2R}$ would be possible from $A_\phi$ for cm energy of 14 TeV at the LHC with integrated luminosities of $10\,\mathrm{fb}^{-1}$ respectively. For $\mathrm{Im}f_{2R}$ the corresponding limit is $\pm 0.050$. $A_{E_\ell}$, which is the most sensitive of the asymmetries we consider, probes $\mathrm{Re}f_{2R}$ and $\mathrm{Im}f_{2R}$ in the ranges $[-0.006, 0.009]$ and $\pm 0.038$ respectively. Limits from $A_b$ are the least stringent, though not much worse than those from $A_{E_\ell}$.

The above results correspond to assuming only one coupling to be nonzero at a time. We also estimated simultaneous limits on $\mathrm{Re}f_{2R}$ and $\mathrm{Im}f_{2R}$ by combining measurements of all observables using a $\chi^2$ analysis. The best possible $1\sigma$ limits on these couplings were found to be $[-0.010, 0.015]$ and $[-0.050, 0.050]$, respectively.

The limits we estimate for LHC with $\sqrt{s} = 7$ TeV and integrated luminosity $1\,\mathrm{fb}^{-1}$ are obviously worse. Nevertheless, they are comparable to those expected from an analysis of $W$ helicities as carried out in [22].

In summary, our proposal provides an alternate place other than top decays to look for anomalous $tbW$ couplings in single-top production where they contribute both in production and in decay. If the contributions of these couplings in the production and in the decay add, then we can have stringent bounds on the couplings, as shown by us in the case of energy distributions. The tW mode is also significant in the probe of these couplings because it does not get any contributions from other new physics like new resonances,

exotic quarks or scalars which could contaminate other single-top production modes and $t\bar{t}$-production process.

Our results would be somewhat worsened by the inclusion realistic detection efficiencies for the $b$ jet and for the detection of the $W$. However, we would like to emphasize that since we do not require accurate reconstruction of the full top-quark four-momentum, the limits are not likely to be much worse. On the other hand, inclusion of the $\bar{t}W^+$ final state, as well as additional leptonic channels in top decay would contribute to improving on our estimates of the limits. A more complete analysis including detector simulation would be worthwhile to carry out.

## Acknowledgments

## A  Spin-density matrix for the process $bg \to tW^-$

In this appendix, we give the spin density matrix elements for the single-top production process. For this we use the following notation for scalar products of four-momenta involved in the process: $(p_t \cdot p_b) = \mathcal{S}_{tb}$, $(p_t \cdot p_g) = \mathcal{S}_{tg}$ and $(p_b \cdot p_g) = \mathcal{S}_{bg}$. Also, we use the following expressions:

$$
\begin{aligned}
\mathcal{F}_1 = \frac{g^2 g_s^2}{24 \mathcal{S}_{tg}^2 \mathcal{S}_{bg}^2} \bigg[ & \left\{ |f_{1L}|^2 \left( 1 + \frac{m_t^2}{2m_W^2} \right) + 3 \mathrm{Re} f_{1L} f_{2R}^* \frac{m_t}{m_W} + 3 |f_{2R}|^2 \frac{m_t^2}{2m_W^2} \right\} \\
& \times \left\{ [\mathcal{S}_{tb} + \mathcal{S}_{tg} - \mathcal{S}_{bg}] \left[ 2 \mathcal{S}_{tg} \mathcal{S}_{tb} \mathcal{S}_{bg} - m_t^2 \mathcal{S}_{bg}^2 \right] - \mathcal{S}_{tg} \mathcal{S}_{bg} \left[ \mathcal{S}_{bg}^2 - \mathcal{S}_{tg}^2 \right] \right\} \\
& - |f_{1L}|^2 \frac{m_t^2}{m_W^2} \mathcal{S}_{tg}^2 \mathcal{S}_{bg}^2 + \mathrm{Re} f_{1L} f_{2R}^* \frac{m_t}{m_W} \left\{ 2 \mathcal{S}_{tg} \mathcal{S}_{bg}^2 [\mathcal{S}_{bg} - \mathcal{S}_{tg}] \right\} \\
& + \frac{|f_{2R}|^2}{m_W^2} \Big\{ m_t^2 [-\mathcal{S}_{bg}^2 (\mathcal{S}_{bg} \mathcal{S}_{tg} - \mathcal{S}_{tb}^2 + \mathcal{S}_{bg}^2)] + \mathcal{S}_{tg} \mathcal{S}_{bg} \big[ \mathcal{S}_{tb} (\mathcal{S}_{tg} + \mathcal{S}_{tb} - \mathcal{S}_{bg}) \\
& \times \{ 3(\mathcal{S}_{bg} - \mathcal{S}_{tg}) - \mathcal{S}_{tb} \} + \{ (\mathcal{S}_{bg} + \mathcal{S}_{tg})(\mathcal{S}_{bg}^2 - \mathcal{S}_{tg}^2) - \mathcal{S}_{tg}^3 \} \big] \Big\} \bigg]
\end{aligned}
$$

$$
\begin{aligned}
\mathcal{F}_2 = \frac{g^2 g_s^2}{12 \mathcal{S}_{tg}^2 \mathcal{S}_{bg}^2} \bigg[ & \left\{ |f_{1L}|^2 \left( 1 - \frac{m_t^2}{2m_W^2} \right) + \mathrm{Re} f_{1L} f_{2R}^* \frac{m_t}{m_W} + |f_{2R}|^2 \frac{m_t^2}{2m_W^2} \right\} m_t \mathcal{S}_{bg} \\
& \times \big[ (\mathcal{S}_{bn} + \mathcal{S}_{gn}) \mathcal{S}_{tg} (\mathcal{S}_{tb} + \mathcal{S}_{tg}) - \mathcal{S}_{bg} (\mathcal{S}_{tb} \mathcal{S}_{gn} + \mathcal{S}_{tg} \mathcal{S}_{bn} + m_t^2 \mathcal{S}_{bn} - \mathcal{S}_{gn}) + \mathcal{S}_{tb} \mathcal{S}_{tg} \mathcal{S}_{bn} \big] \\
& - |f_{1L}|^2 \frac{m_t^2}{m_W^2} \mathcal{S}_{tg} \mathcal{S}_{bg}^2 \mathcal{S}_{gn} + \mathrm{Re} f_{1L} f_{2R}^* \frac{1}{m_W} \left\{ 2 \mathcal{S}_{tg}^2 \mathcal{S}_{bg} [\mathcal{S}_{tb} \mathcal{S}_{gn} - \mathcal{S}_{tg} \mathcal{S}_{bn}] \right\} \\
& + |f_{2R}|^2 \Big\{ \mathcal{S}_{bn} (\mathcal{S}_{tb} - \mathcal{S}_{bg} + \mathcal{S}_{tg})(m_t^2 \mathcal{S}_{bg}^2 - 3 \mathcal{S}_{bg} \mathcal{S}_{tg}^2 + \mathcal{S}_{bg}^2 \mathcal{S}_{tg} - 2 \mathcal{S}_{bg} \mathcal{S}_{tg} \mathcal{S}_{tb}) \\
& + 2 \mathcal{S}_{bg} \mathcal{S}_{tg}^2 \mathcal{S}_{tb} + \mathcal{S}_{gn} (\mathcal{S}_{tb} - \mathcal{S}_{bg} - \mathcal{S}_{tg})(-\mathcal{S}_{bg} \mathcal{S}_{tg} \mathcal{S}_{tb} + \mathcal{S}_{bg} \mathcal{S}_{tg}^2 - \mathcal{S}_{bg}^3) - 2 \mathcal{S}_{bg} \mathcal{S}_{tg}^3 \\
& + \mathcal{S}_{bg}^2 (\mathcal{S}_{tb} \mathcal{S}_{bg} + 2 \mathcal{S}_{bg} \mathcal{S}_{tg} + \mathcal{S}_{bg}^2 + m_t^2 \mathcal{S}_{tg}) \Big\} \bigg]
\end{aligned}
$$

The diagonal elements of the spin density matrix for single-top production in $tW$ channel can be written as

$$\rho(\pm, \pm) = \mathcal{F}_1 \pm \mathcal{F}_2 \tag{A.1}$$

with $\mathcal{S}_{gn} = (p_g.n_3)$ and $\mathcal{S}_{bn} = (p_b.n_3)$ and the off-diagonal elements are

$$\rho(\pm, \mp) = \mathcal{F}_2 \tag{A.2}$$

with $\mathcal{S}_{gn} = (p_g.(n_1 \pm in_2))$ and $\mathcal{S}_{bn} = (p_b.(n_1 \pm in_2))$ where $n_i^\mu$'s $(i = 1, 2, 3)$ are the four-vectors with the properties $n_i \cdot n_j = -\delta_{ij}$ and $n_i \cdot p_t = 0$. $n_1$, $n_2$ and $n_3$ represent spin four-vectors of the top quark with spin respectively along the $x$, $y$ and $z$ axis in the top rest frame.

## References

[1] CDF collaboration, F. Abe et al., *Evidence for top quark production in $\bar{p}p$ collisions at $\sqrt{s} = 1.8\ TeV$*, *Phys. Rev. Lett.* **73** (1994) 225 [hep-ex/9405005] [INSPIRE].

[2] CDF AND D0 collaboration, *A Combination of CDF and D0 results on the mass of the top quark*, hep-ex/0703034 [INSPIRE].

[3] I.I. Bigi, Y.L. Dokshitzer, V.A. Khoze, J.H. Kuhn and P.M. Zerwas, *Production and Decay Properties of Ultraheavy Quarks*, *Phys. Lett.* **B 181** (1986) 157 [INSPIRE].

[4] K. Huitu, S. Kumar Rai, K. Rao, S.D. Rindani and P. Sharma, *Probing top charged-Higgs production using top polarization at the Large Hadron Collider*, *JHEP* **04** (2011) 026 [arXiv:1012.0527] [INSPIRE].

[5] M. Arai, K. Huitu, S.K. Rai and K. Rao, *Single production of sleptons with polarized tops at the Large Hadron Collider*, *JHEP* **08** (2010) 082 [arXiv:1003.4708] [INSPIRE].

[6] R.M. Godbole, K. Rao, S.D. Rindani and R.K. Singh, *On measurement of top polarization as a probe of $t\bar{t}$ production mechanisms at the LHC*, *JHEP* **11** (2010) 144 [arXiv:1010.1458] [INSPIRE].

[7] D. Choudhury, R.M. Godbole, S.D. Rindani and P. Saha, *Top polarization, forward-backward asymmetry and new physics*, *Phys. Rev.* **D 84** (2011) 014023 [arXiv:1012.4750] [INSPIRE].

[8] E.L. Berger, Q.-H. Cao, C.-R. Chen and H. Zhang, *Top Quark Polarization As A Probe of Models with Extra Gauge Bosons*, *Phys. Rev.* **D 83** (2011) 114026 [arXiv:1103.3274] [INSPIRE].

[9] A. Heinson, A. Belyaev and E. Boos, *Single top quarks at the Fermilab Tevatron*, *Phys. Rev.* **D 56** (1997) 3114 [hep-ph/9612424] [INSPIRE].

[10] T. Stelzer, Z. Sullivan and S. Willenbrock, *Single top quark production at hadron colliders*, *Phys. Rev.* **D 58** (1998) 094021 [hep-ph/9807340] [INSPIRE].

[11] A. Belyaev, E. Boos and L. Dudko, *Single top quark at future hadron colliders: Complete signal and background study*, *Phys. Rev.* **D 59** (1999) 075001 [hep-ph/9806332] [INSPIRE].

[12] E. Boos, L. Dudko and T. Ohl, *Complete calculations of $Wb\bar{b}$ and $Wb\bar{b}$ + jet production at Tevatron and LHC: Probing anomalous $Wtb$ couplings in single top production*, *Eur. Phys. J.* **C 11** (1999) 473 [hep-ph/9903215] [INSPIRE].

[13] T.M. Tait, *The tW⁻ mode of single top production*, *Phys. Rev.* **D 61** (2000) 034001 [hep-ph/9909352] [INSPIRE].

[14] D. Espriu and J. Manzano, *Measuring effective electroweak couplings in single top production at the LHC*, *Phys. Rev.* **D 65** (2002) 073005 [hep-ph/0107112] [INSPIRE].

[15] D. Espriu and J. Manzano, *A Study of top polarization in single top production at the CERN LHC*, *Phys. Rev.* **D 66** (2002) 114009 [hep-ph/0209030] [INSPIRE].

[16] T.M. Tait and C.-P. Yuan, *Single top quark production as a window to physics beyond the standard model*, *Phys. Rev.* **D 63** (2000) 014018 [hep-ph/0007298] [INSPIRE].

[17] THE CDF collaboration, T. Aaltonen et al., *Measurement of W-Boson Polarization in Top-quark Decay in ppbar Collisions at $\sqrt{s} = 1.96\,TeV$*, *Phys. Rev. Lett.* **105** (2010) 042002 [arXiv:1003.0224] [INSPIRE].

[18] D0 collaboration, V.M. Abazov et al., *Measurement of the W boson helicity in top quark decays using $5.4\,fb^{-1}$ of $p\bar{p}$ collision data*, *Phys. Rev.* **D 83** (2011) 032009 [arXiv:1011.6549] [INSPIRE].

[19] C.-R. Chen, F. Larios and C.-P. Yuan, *General analysis of single top production and W helicity in top decay*, *Phys. Lett.* **B 631** (2005) 126 [hep-ph/0503040] [INSPIRE].

[20] ATLAS collaboration, G. Aad et al., *Measurement of the W-boson polarisation in top quark decays in pp collision data at $\sqrt{s} = 7\,TeV$ using the ATLAS detector*, ATLAS-CONF-2011-037 (2011).

[21] CMS collaboration, S. Chatrchyan et al., *Measurement of the Polarization of W Bosons with Large Transverse Momenta in W+Jets Events at the LHC*, *Phys. Rev. Lett.* **107** (2011) 021802 [arXiv:1104.3829] [INSPIRE].

[22] J. Aguilar-Saavedra, N. Castro and A. Onofre, *Constraints on the Wtb vertex from early LHC data*, *Phys. Rev.* **D 83** (2011) 117301 [arXiv:1105.0117] [INSPIRE].

[23] C.D. White, S. Frixione, E. Laenen and F. Maltoni, *Isolating Wt production at the LHC*, *JHEP* **11** (2009) 074 [arXiv:0908.0631] [INSPIRE].

[24] S. Frixione, E. Laenen, P. Motylinski, B.R. Webber and C.D. White, *Single-top hadroproduction in association with a W boson*, *JHEP* **07** (2008) 029 [arXiv:0805.3067] [INSPIRE].

[25] S. Frixione, E. Laenen, P. Motylinski and B.R. Webber, *Single-top production in MC@NLO*, *JHEP* **03** (2006) 092 [hep-ph/0512250] [INSPIRE].

[26] CMS collaboration, S. Chatrchyan et al., *Measurement of the t-channel single top quark production cross section in pp collisions at $\sqrt{s} = 7\,TeV$*, *Phys. Rev. Lett.* **107** (2011) 091802 [arXiv:1106.3052] [INSPIRE].

[27] J. Aguilar-Saavedra, J. Carvalho, N.F. Castro, F. Veloso and A. Onofre, *Probing anomalous Wtb couplings in top pair decays*, *Eur. Phys. J.* **C 50** (2007) 519 [hep-ph/0605190] [INSPIRE].

[28] W. Bernreuther, P. Gonzalez and M. Wiebusch, *The Top Quark Decay Vertex in Standard Model Extensions*, *Eur. Phys. J.* **C 60** (2009) 197 [arXiv:0812.1643] [INSPIRE].

[29] P.L. Cho and M. Misiak, *$b \to s\gamma$ decay in $\mathrm{SU}(2)_L \times \mathrm{SU}(2)_R \times \mathrm{U}(1)$ extensions of the Standard Model*, *Phys. Rev.* **D 49** (1994) 5894 [hep-ph/9310332] [INSPIRE].

[30] F. Larios, M. Perez and C. Yuan, *Analysis of tbW and ttZ couplings from CLEO and LEP/SLC data*, *Phys. Lett.* **B 457** (1999) 334 [hep-ph/9903394] [INSPIRE].

[31] G. Burdman, M. Gonzalez-Garcia and S. Novaes, *Anomalous couplings of the third generation in rare B decays*, *Phys. Rev.* **D 61** (2000) 114016 [hep-ph/9906329] [INSPIRE].

[32] B. Grzadkowski and M. Misiak, *Anomalous Wtb coupling effects in the weak radiative B-meson decay*, *Phys. Rev.* **D 78** (2008) 077501 [arXiv:0802.1413] [INSPIRE].

[33] J. Drobnak, S. Fajfer and J.F. Kamenik, *Interplay of $t \to bW$ Decay and $B_q$ Meson Mixing in Minimal Flavor Violating Models*, *Phys. Lett.* **B 701** (2011) 234 [arXiv:1102.4347] [INSPIRE].

[34] B. Grzadkowski and Z. Hioki, *New hints for testing anomalous top quark interactions at future linear colliders*, *Phys. Lett.* **B 476** (2000) 87 [hep-ph/9911505] [INSPIRE].

[35] S.D. Rindani, *Effect of anomalous t b W vertex on decay lepton distributions in $e^+e^- \to t\bar{t}$ and CP-violating asymmetries*, *Pramana* **54** (2000) 791 [hep-ph/0002006] [INSPIRE].

[36] B. Grzadkowski and Z. Hioki, *Angular distribution of leptons in general $t\bar{t}$ production and decay*, *Phys. Lett.* **B 529** (2002) 82 [hep-ph/0112361] [INSPIRE].

[37] B. Grzadkowski and Z. Hioki, *Decoupling of anomalous top decay vertices in angular distribution of secondary particles*, *Phys. Lett.* **B 557** (2003) 55 [hep-ph/0208079] [INSPIRE].

[38] Z. Hioki, *Probing anomalous top couplings through the final lepton angular and energy distributions at polarized NLC*, hep-ph/0104105 [INSPIRE].

[39] Z. Hioki, *A New decoupling theorem in top quark physics*, hep-ph/0210224 [INSPIRE].

[40] K. Ohkuma, *Effects of top quark anomalous decay couplings at $\gamma\gamma$ colliders*, *Nucl. Phys. Proc. Suppl.* **111** (2002) 285 [hep-ph/0202126] [INSPIRE].

[41] R.M. Godbole, S.D. Rindani and R.K. Singh, *Lepton distribution as a probe of new physics in production and decay of the t quark and its polarization*, *JHEP* **12** (2006) 021 [hep-ph/0605100] [INSPIRE].

[42] M. Beccaria, F.M. Renard and C. Verzegnassi, *Electroweak supersymmetric effects on high energy unpolarized and polarized single top production at CERN LHC*, *Phys. Rev.* **D 71** (2005) 033005 [hep-ph/0410089] [INSPIRE].

[43] J. Vermaseren, *New features of FORM*, math-ph/0010025 [INSPIRE].

[44] J. Pumplin, A. Belyaev, J. Huston, D. Stump and W. Tung, *Parton distributions and the strong coupling: CTEQ6AB PDFs*, *JHEP* **02** (2006) 032 [hep-ph/0512167] [INSPIRE].

[45] W. Bernreuther, *Top quark physics at the LHC*, *J. Phys.* **G 35** (2008) 083001 [arXiv:0805.1333] [INSPIRE].

[46] F. Hubaut, E. Monnier, P. Pralavorio, K. Smolek and V. Simak, *ATLAS sensitivity to top quark and W boson polarization in $t\bar{t}$ events*, *Eur. Phys. J.* **C 44S2** (2005) 13 [hep-ex/0508061] [INSPIRE].

[47] J. Aguilar-Saavedra, J. Carvalho, N.F. Castro, A. Onofre and F. Veloso, *ATLAS sensitivity to Wtb anomalous couplings in top quark decays*, *Eur. Phys. J.* **C 53** (2008) 689 [arXiv:0705.3041] [INSPIRE].

[48] J. Aguilar-Saavedra, *Single top quark production at LHC with anomalous Wtb couplings*, *Nucl. Phys.* **B 804** (2008) 160 [arXiv:0803.3810] [INSPIRE].

[49] J. Aguilar-Saavedra and J. Bernabeu, *W polarisation beyond helicity fractions in top quark decays*, *Nucl. Phys.* **B 840** (2010) 349 [arXiv:1005.5382] [INSPIRE].

[50] M.M. Najafabadi, *Probing of Wtb Anomalous Couplings via the tW Channel of Single Top Production*, *JHEP* **03** (2008) 024 [arXiv:0801.1939] [INSPIRE].

[51] A. Lucotte, A. Lléres and D. Chevallier, ATLAS note ATL-PHYS-PUB-2007-005.

[52] S. Zhu, *Next-to-leading order QCD corrections to bg → tW⁻ at CERN large hadron collider*, hep-ph/0109269 [INSPIRE].

[53] M. Beccaria et al., *A Complete one-loop description of associated tW production at LHC and a search for possible genuine supersymmetric effects*, *Eur. Phys. J.* **C 53** (2008) 257 [arXiv:0705.3101] [INSPIRE].